

Living Room Model

Sjaak Uitterdijk

Abstract

By presenting the relevant, in relation to the climate problem, measured variables as exponential functions, truthfully representing the real values, surprising informative mutual relations show up. One of these relations led to the successful investigation of the possibility that the global temperature raise can not be caused by indirect heating, prescribed by the Green House model, but is caused by direct heating, prescribed by the here named Living Room Model. It is of fundamental importance to realize that sun, wind and earth energy that is transformed to energy, intended to be consumed by mankind, also directly heats the atmosphere. Besides that it has been proven that the Sea is heated by the geothermal heat flux. The final outcome therefore is that aiming for reduced CO₂ emissions will not result in any improvement of the climate. Only a drastically reduction of the consumed energy, of whichever kind, will help.

Copyright © November 2021 Sjaak Uitterdijk

Author: Sjaak Uitterdijk

Print: Pumbo.nl

Cover design: Sjaak Uitterdijk / Pumbo.nl

Interior design: Sjaak Uitterdijk

Publisher: SJU

Climate Research

NUR-code: 600

ISBN/EAN: 978-94-6406-738-5

Provided the source is mentioned, everything from this book may be copied.

Edition 2

In this edition only the chapters of edition 1 have been rearranged.

*If humanity would cease to exist overnight, the temperature of the atmosphere
would return to the level of 150 years ago
in about one week's time.*

Prologue

One of the original objections to the Greenhouse Model is the conflicting observation that it happened the last 200 years four times that the global temperature dropped while the CO₂ concentration in the atmosphere kept rising.

To support this opinion more scientifically, a special mathematical operation has been applied to the very noise-like graph of the global temperature, which filters out all that noise, but preserves the essence. The result was even a much more clear contradiction between global temperature and CO₂ concentration.

However the graph of the global temperature also shows a long-term increase, having a strong correlation with the CO₂ concentration in the atmosphere.

Eventually it has been made clearly visible that a precise sinusoidal (64-year period) change is the cause of what led originally to the conflicting observations. This yet incomprehensible periodical phenomenon has to be considered as a completely independent part of the long-term increasing global temperature.

As a result the aforementioned long-term correlation now strongly tempts the observer to consider the increasing CO₂ concentration in the atmosphere as the cause of its increasing temperature. However, a correlation does not necessarily mean a causation.

Studying the basic principle of the Greenhouse Model led to the conclusion that the alleged difference between the incoming radiation of the Sun during day-time and the outgoing radiation during night-time has been adapted to the heat power density, necessary to heat the Sea (all oceans and seas together) in conformity to what has been measured. What has actually been measured is an increase of the temperature, at the surface being equal to the increase in the atmosphere. This increase is diminishing with depth to zero at a few kilometres depth. The related increase of the Sea's heat energy has now been calculated from the measured increased temperature and used as argument in favour of the Greenhouse Model. However, there is no evidence whatsoever for the alleged relation between the difference of incoming and outgoing radiation and the rise of atmosphere's temperature.

Besides this misleading presentation it can be proven that the heating of the Sea, decreasing with depth, can not be caused, as assumed in the Greenhouse Model, by a top down heating, whether directly by the mentioned radiation, or indirectly via the atmosphere. Such a result can only be achieved by a bottom up heating. The most obvious solution turns out to be the million years old natural geothermal heat flow. In a way just like the water level in the estuary of a river enhances with the tide of the sea into which it flows. And it also resembles very well the phenomenon that the further inland, the less remains in the river of that elevated level in the estuary.

Based on the physical law that prescribes that all consumed energy is fully converted into heat, the idea arose that the increase of atmosphere's temperature could, in principle, be caused by direct heating due to the consumed energy by mankind, in this book called Living Room Model.

The theoretical research into the relationship between consumed energy and global warming, together with several fundamental objections to the Greenhouse Model, leads to the conclusion that the Greenhouse Model has to be rejected in favour of the Living Room Model.

With this model the so-called Hot Spots on Earth can perfectly explained too.

Contents

I	Mathematical expression for the CO ₂	1
II	Mathematical expression for the global temperature	2
	II.1 Short-term-trend	
	II.2 Long-term-trend	
	II.3 Interesting spin-off	
III	Mathematical expression for the world population	5
IV	Mathematical expression for the worldwide energy consumption	6
V	Consideration of cause and effect	7
VI	Investigation of the increased Sea heat energy	8
VII	Why the Greenhouse Model is untenable	10
	VII.1 Introduction	
	VII.2 Principle of the GHM	
	VII.3 A closer look at spectra	
	VII.4 A closer look at the heat fluxes of the GHM	
	VII.5 The heating of the Sea in the GHM	
	VII.6 The GHM applied on Mars and Venus	
	VII.7 The Reverse Greenhouse Effect	
VIII	Living Room Model	18
	VIII.1 Introduction	
	VIII.2 Heat balance of the atmosphere	
	VIII.3 The heating of the atmosphere in the LRM	
	VIII.4 LRM heating since 1810	
	VIII.5 The heating of the Sea in the LRM	
	VIII.6 Hot Spots on Earth	
IX	Monthly global temperature and CO ₂ anomalies	22
X	Global Mean Sea Level until 2100	26
	X.1 Introduction	
	X.2 Mathematical expression for CSIRO measurements	
	Conclusions	27
	Appendix 1 Mathematical background of the polynomial and exponential curve fitting	28
	Appendix 2 Calculation of the heat capacity of the atmosphere	30
	Appendix 3 Impact of sustainable energy	32
	Appendix 4 The World Population in the Past and in the Future	33
	Epilogue	36
	References	37

I Mathematical expression for the CO₂

From here on, for simplicity's sake, the variable "CO₂ concentration in the atmosphere" will be called: CO₂. The CO₂ measurements, as presented in reference [I], are called: Monthly Mean Concentrations at the Mauna Loa Observatory. For the purpose of this investigation their monthly registrations are transformed to yearly mean values. The measurements have been carried out since 1958. The units are in parts per million or ppm.

The graphs of these measurements show a very smooth tendency, hardly possessing random deviations and are therefore very suitable for applying the curve fitting $y = c + a \cdot \exp(t/b)$. See Appendix 1.2. The outcome, based on the measurements in the years 1958, 1986 and 2014, is:

$$\text{CO}_2(t) = 259.4 + 6.60 \cdot 10^{-13} \cdot \exp(t/61.06)$$

Taking $b = 61$, $c = 259$ and $a = 6.4 \cdot 10^{-13}$, learns that hardly any deviation can be found in the graph in fig. I.1.

Therefore the mathematical expression for the concentration of the CO₂ is chosen as:

$$\text{CO}_2(t) = 259 + 6.4 \cdot 10^{-13} \cdot \exp(t/61) \quad \text{ppm} \quad (1)$$

In this function the variable t is the actual year number, which explains the small value of the constant a . Based on the fact that the calculated curve shows an excellent fit with the measurements, it is considered justifiable to extrapolate the values back to 1850.

1850 is the year in which the recording of the *global temperature*, to be considered hereafter, was started.

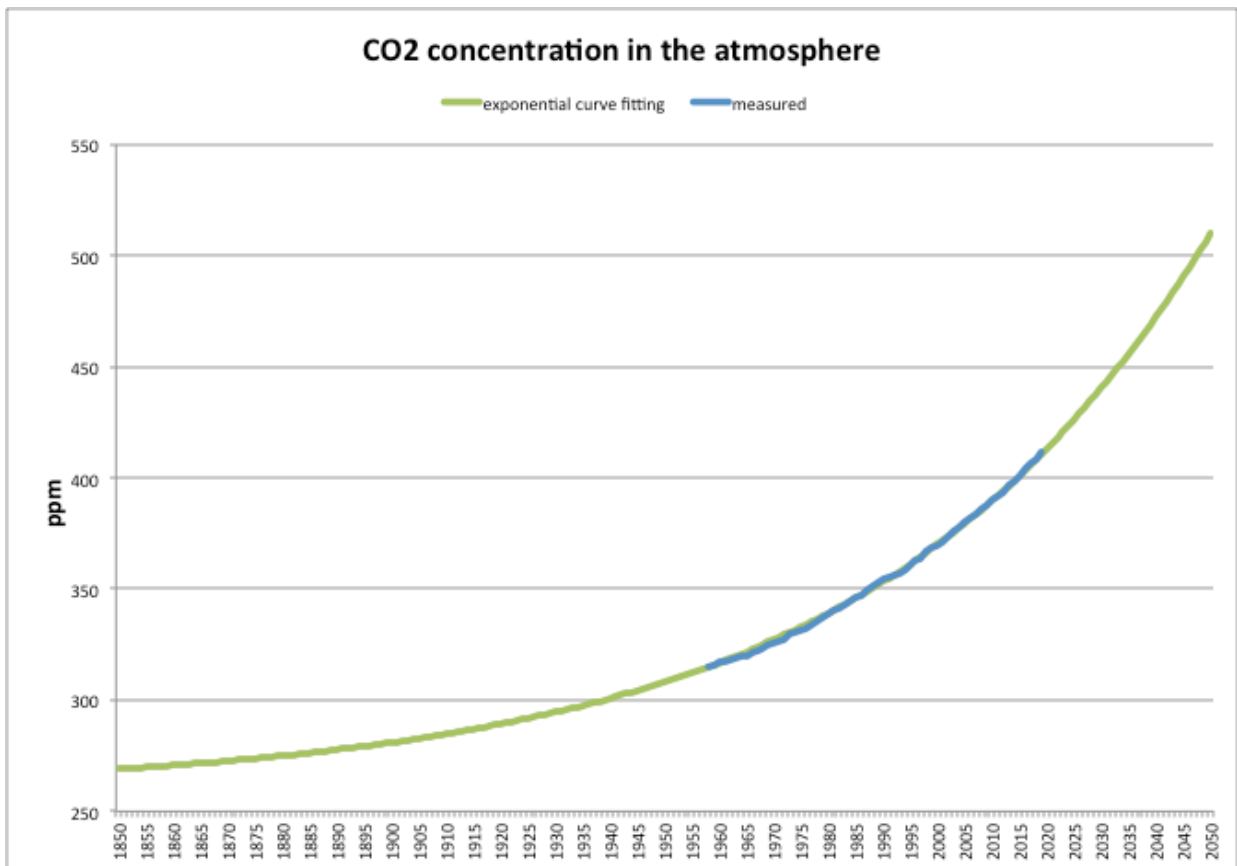


Figure I.1: Measured CO₂ since 1958 and fitted curve extrapolated back to 1850 and forward to 2050

II Mathematical expression for the global temperature

II.1 Definition of the global temperature

The global temperature is calculated as the average temperature, measured in a few thousand stations throughout the world. The measurements take place at a height of 1.5 to 2 meters above Earth's surface. The global temperature is therefore the temperature of the atmosphere at that height. For that reason, the heat capacity of the atmosphere is considered to be the most crucial parameter in the following assessments. From now on the variable 'global temperature' will be used to express the *yearly mean* value of the measurements.

II.2 Short-term-trend

The measurements of the global temperature had been downloaded around 2015 from a site called: National Aeronautics and Space Administration, Goddard Institute for Space Studies, showing measurements starting in 1850. However the link to that site has been removed. The new link (reference [II]) now shows measurements starting in 1880. The measurements since 1850 have been used for the fitting described below. The measurements have been fitted to an 8th and 9th order polynomial, shown in figure II.1. See Appendix 1.1 for the mathematical background. Considering the mutual rather divergent behaviour, between the 8th and 9th order curves, *only during the last five years*, the mean value of these two polynomials has been calculated and applied as the final high order polynomial fitting.

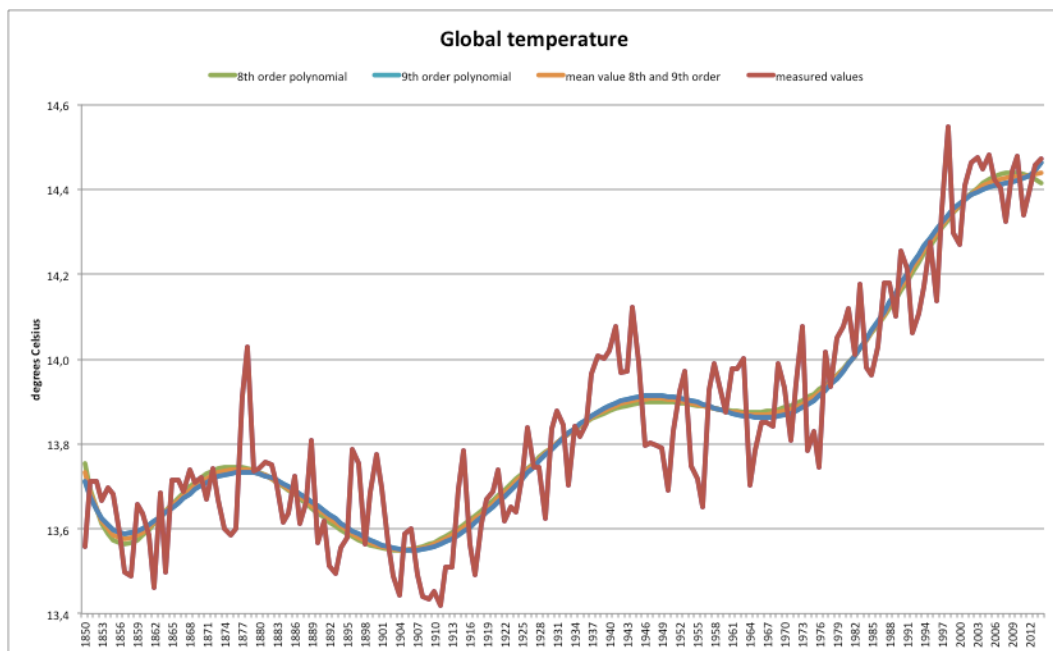


Figure II.1: Global temperature, measured and polynomial fitted

Over the past 10 years, the global temperature no longer significantly increased (0.03 °C), despite the ongoing increase of the CO₂ concentration, as presented above. This means that, assuming the Greenhouse theory is correct, seemingly other processes determine the global temperature too.

This conclusion is supported by the observation that during the periods 1945-1965, 1875-1905 and ? - 1855 this temperature even decreased notwithstanding the always increasing CO₂ concentration.

So it might even be that the Greenhouse theory is not correct, with the consequence that the CO₂ concentration in the atmosphere is not responsible for the increase of the global temperature. To investigate this in more detail a long-term-trend of the global temperature only has to be extracted.

* The question mark concerns data that started in 1834, but this data is not found at Internet anymore since about 2017.

II.3 Long-term-trend

In order to extract a pure long-term-trend of the global temperature, in first instance a 2nd order polynomial fitting has been carried out. See figure II.2. The result shows an unrealistic trend in the first four decades. To eliminate this, the curve fitting $y = c + a \cdot \exp(t/b)$ has been applied to 3 places where the 2nd order polynomial equals the high order polynomial. That means the years 1892, 1958 and 2012.

At the same time it is investigated whether the curvature of the CO₂, to read as the value of b, can be used.

Figure II.2 shows the graph of the function:

$$T_G(t) = 13.5 + 4.4 \cdot 10^{-15} \cdot \exp(t/61) \quad ^\circ\text{C} \quad (2)$$

No reason can be assigned to reject such a curvature, starting at 1890.

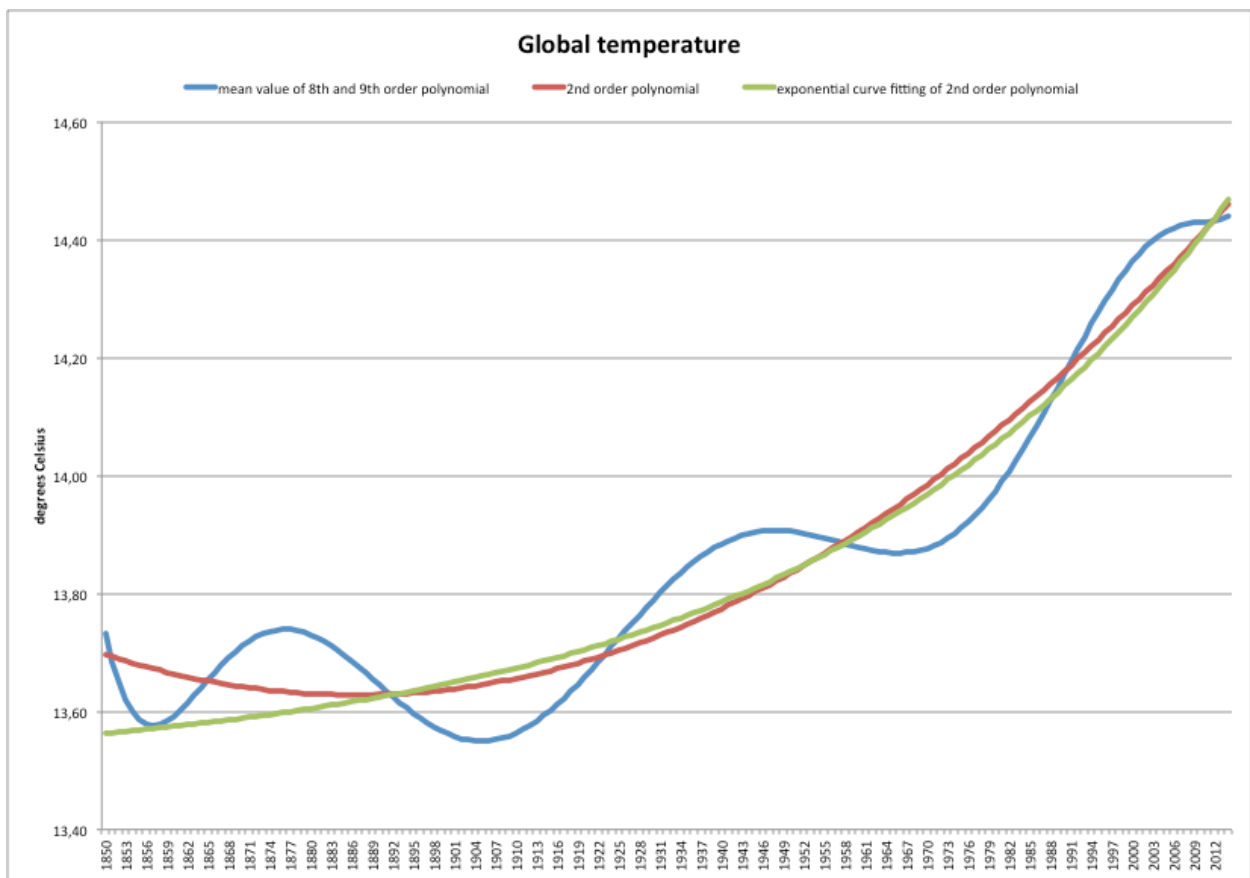


Figure II.2: Global temperature, polynomial and curve fitted, as function of time

II.3 Interesting spin-off

If in figure II.2 the (green) *exponentially fitted* long-term-trend curve is subtracted from the total (blue) curve, a surprising periodical curve results, except for the first period. See the blue curve in fig II.3.

If in figure II.2 the (red) *second order polynomial fitted* long-term-trend curve is subtracted from the total curve a more perfect sinusoidal function remains. See the red curve in fig II.3.

Both curves in figure II.3 show 2.5 periods in 160 years, resulting in 64 years per period.

The curves prove that the actual amplitude of this periodic function is most likely rather precise 0.1 °C.

N.B. The remarkable upwards trend during the first period of the blue curve in figure II.3 might be the reason for withdrawing the data of 1850–1880 from Internet. This data has been available until roughly 2016.

Both periodic functions in figure II.3 have been extrapolated from the year 2012 until 2100 by applying the function: $-A \sin\{\omega(t - 2012)\}$, with $\omega = 2\pi/64$, and $A = 0.1$ °C.

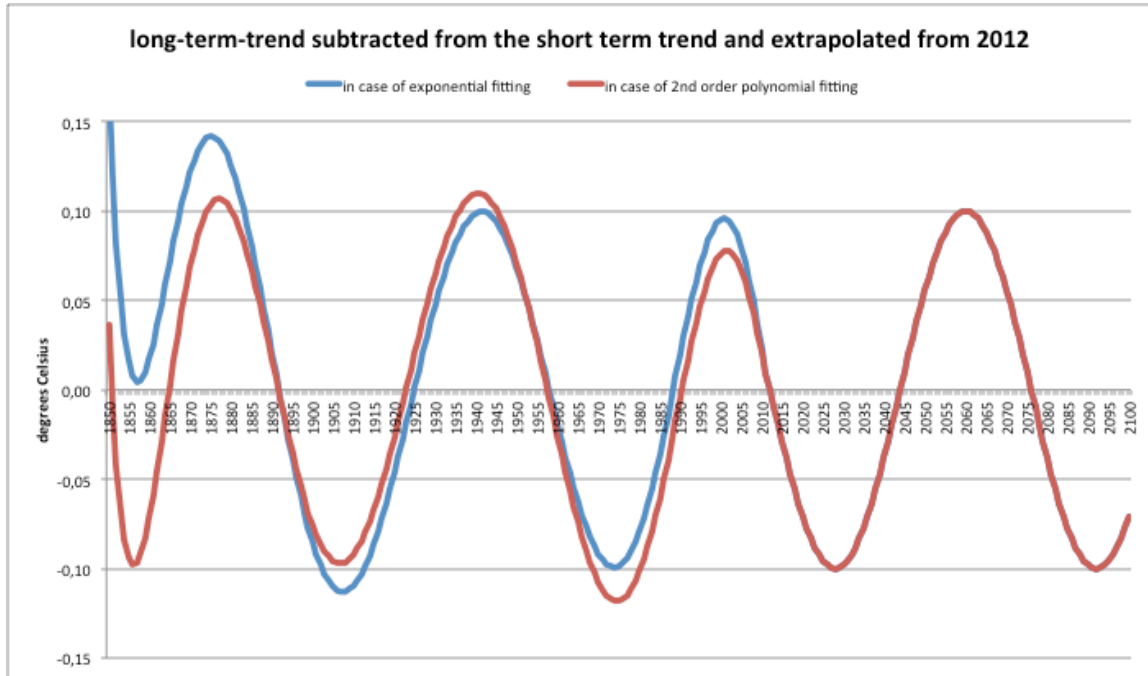


Figure II.3: Periodic functions extrapolated from 2012 with $-0.1 \sin\{\omega(t - 2012)\}$

Doing so, the global temperature increase can be predicted precisely for a long time, shown in figure II.4.

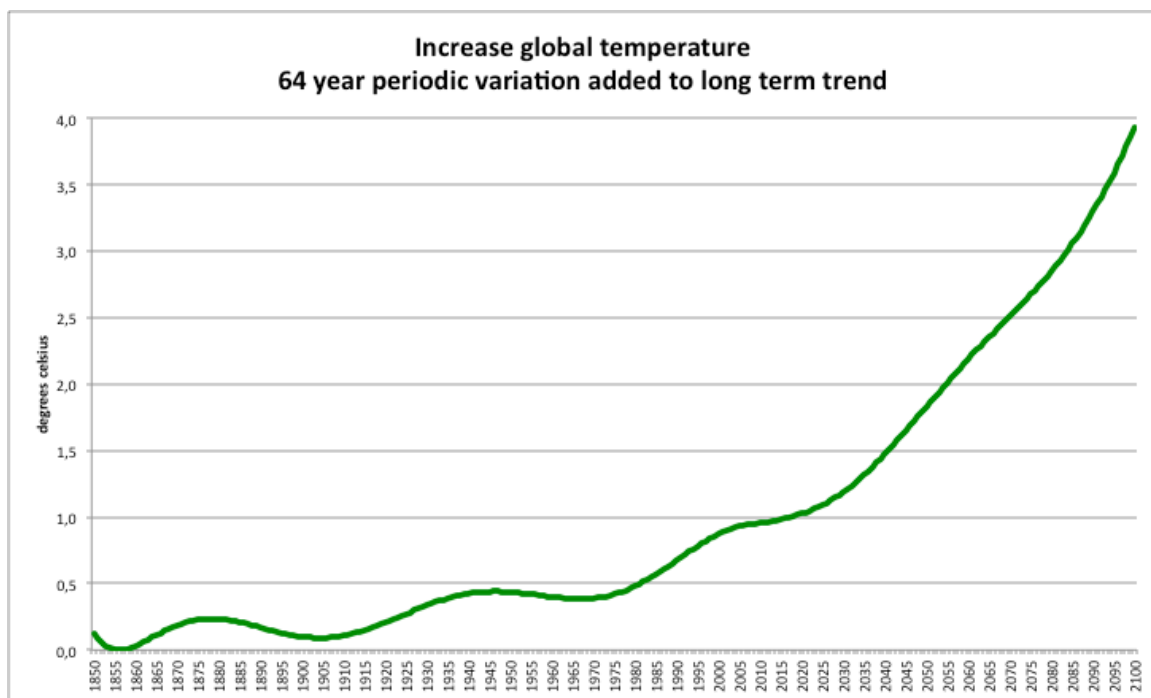


Figure II.4: Predicted increase global temperature (°C) until 2100, including the periodical variations

III Mathematical expression for the world population

There are several sources at the Internet informing about this subject. The world population as shown in reference [III] has been taken as the first approximation. “As a first approximation”, because the graph has such an unnatural character that it is impossible to qualify it as correct:

- an artificial nod in 1925 as well as in 1950,
- in between the two nod and from 1800 to 1925 a straight line.

In order to obtain a more credible curve, which means: as belonging to a natural process, the exponential curve $y = c + a \cdot \exp(t/b)$ is chosen. The value of b is, in advance, taken 61.

The two artificial nod have been eliminated by using the inputs belonging to 2014 and 1914. The result is:

$$W_p(t) = 0.47 + 3.2 \cdot 10^{-14} \cdot \exp(t/61) \quad [\text{billion}] \quad (3)$$

Figure III.1 proves that this is most likely an entirely acceptable representation of reality.

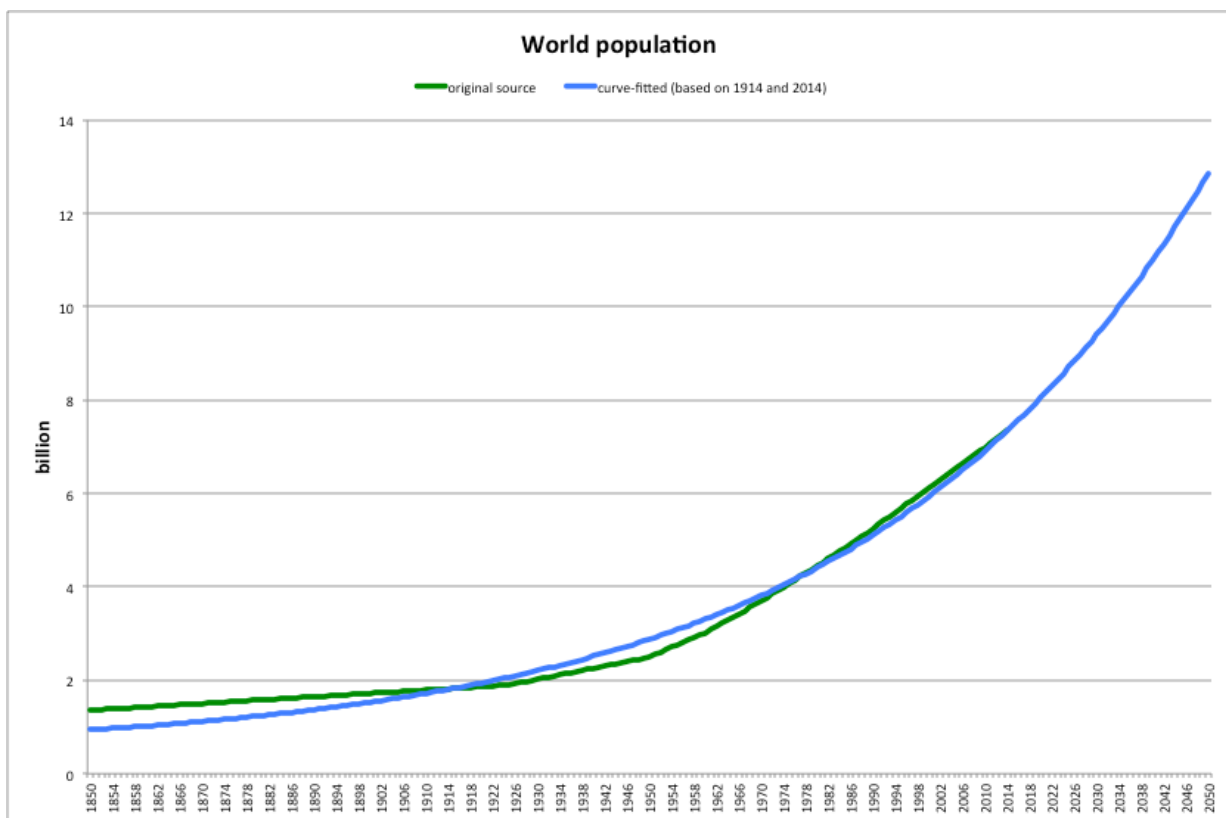


Figure III.1: The world population as function of time: the original and the most likely curve

Formula (3) expresses that such a growth will lead to a world population of 29 billion in 2100!

IV Mathematical expression for the worldwide energy consumption

Global administrations of the consumption of fossil fuels has led to the graph of the annual energy consumption in the past 200 years, shown in figure IV.1. The figure has been copied from reference [IV].

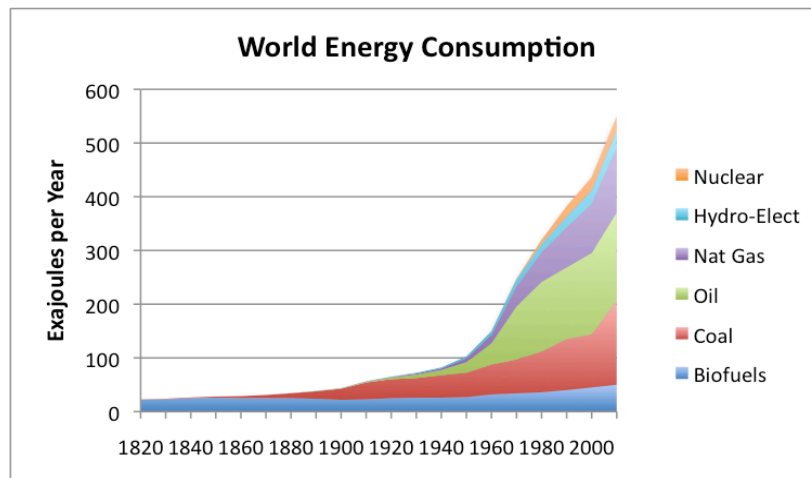


Figure IV.1 World Energy Consumption by Source, Based on Vaclav Smil estimates from Energy Transitions

The graph shows “humps” and “dents” conflicting with the streamlined graph of the measured and backwards extrapolated CO₂ concentration in the atmosphere, shown in chapter I. For this reason this graph has also been streamlined by means of exponential curve-fitting.

The data has first been converted to a stylized graph and at the same time to TeraWatt (TW), applying the relation: 1 Exajoule/year = $10^{18} / (3600 \cdot 24 \cdot 365) \text{ W} = 0.0317 \text{ TW}$. See the blue curve in figure IV.2.

The years 2010 and 1810 have been taken as references for the curve fitting. The time constant (b) is, in advance, taken 61 year. The result is: $P_G(t) = -0.06 + 8.4 \cdot 10^{-14} \cdot \exp(t/61)$. The value -0.06 is not realistic, but small enough to be ignored. So the globally applied power, expressed in TW, will be written as:

$$P_G(t) = 8.4 \cdot 10^{-14} \cdot \exp(t/61) \text{ TW} \quad (4)$$

Figure IV.2 shows the related graphs and also that, without compromising credibility, the curvature of the applied power graph may be chosen as 61. The legitimate question namely is how reliable these registrations were until the discovery of the climate problem!

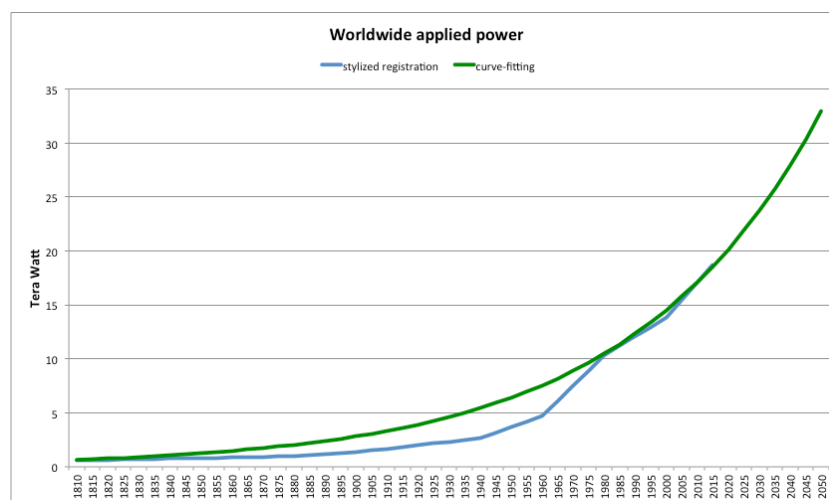


Figure IV.2. Worldwide power usage from 1810 to 2050

V Consideration of cause and effect

It has been shown in the previous chapters that the four variables: CO₂ concentration, global temperature, world population and globally applied power, can all reasonably be expressed as function of time by an exponential function with time constant 61 years:

$$\text{CO}_2 \text{ concentration} \quad \text{ppm} \quad \text{CO}_2(t) = 259 + 6.4 \cdot 10^{-13} \cdot \exp(t/61) \quad (1)$$

$$\text{Global temperature} \quad ^\circ\text{C} \quad T_G(t) = 13.5 + 4.4 \cdot 10^{-15} \cdot \exp(t/61) \quad (2)$$

$$\text{World population} \quad \text{billion} \quad W_p(t) = 0.5 + 3.2 \cdot 10^{-14} \cdot \exp(t/61) \quad (3)$$

$$\text{Globally applied power} \quad \text{TW} \quad P_G(t) = 8.4 \cdot 10^{-14} \cdot \exp(t/61) \quad (4)$$

The mutual relations between these variables can be deduced as shown below by means of the example, showing the Greenhouse model.

$$\text{CO}_2(t) - 259 = 6.4 \cdot 10^{-13} \cdot \exp(t/61)$$

$$T_G(t) - 13.5 = 4.4 \cdot 10^{-15} \cdot \exp(t/61)$$

so

$$\{T_G(t) - 13.5\} / \{\text{CO}_2(t) - 259\} = 4.4 \cdot 10^{-15} / 6.4 \cdot 10^{-13} = 7 \cdot 10^{-3} \text{ resulting in:}$$

$$\text{global temperature} = 13.5 + 0.007 \cdot (\text{CO}_2 - 259)$$

This expression written inversely shows:

$$\text{CO}_2 = 259 + 145 \cdot (\text{global temperature} - 13.5)$$

In the first expression the CO₂ is meant as the cause and the temperature as the effect, while the second one suggests the opposite. So the interpretation of such relationships requires a careful consideration.

For example, might it be that the world population is *directly* responsible for the global warming, given the relation

$$\text{global temperature} = 13.5 + 0.14 \cdot (\text{population} - 0.5)$$

Or is that population indirectly responsible, via its energy consumption:

$$\text{global temperature} = 13.5 + 0.05 \cdot \text{Globally applied power}$$

In chapter VII it will be shown that and why the Greenhouse Model is untenable. One of the reasons is that this model assumes a *top down* heating until great depth of the Sea. The word "Sea" is used to express all the oceans and seas together. In order to explain that such a process is physically impossible, it is firstly necessary to investigate this heating. See the next chapter.

After having proven that the Greenhouse Model is untenable it will be proven in chapter VIII that the global warming is the result of the globally applied power by mankind, referred to with the name Living Room Model. Its density, in terms of Watt/m², is much lower than the alleged density of the Greenhouse Model. That is to say: this alleged density has never been measured but adapted to the density necessary to heat the Sea top down. It will be shown that an unexpected source is responsible for the heating of the Sea, *bottom up*.

Finally: the so-called phenomenon Hot Spot can not be explained by the Greenhouse Model. In the last section of chapter VIII it will be shown that the Living Room Model perfectly explains this phenomenon.

VI Investigation of the increased Sea heat energy

Two sources have been investigated in order to find reliable information about the amount of the increased heat energy in the Sea (all oceans and seas together). Figure VI.1 is a copy of figure 6 from reference [VI.1]. Figure VI.2 is a copy of page 10 from reference [VI.2].

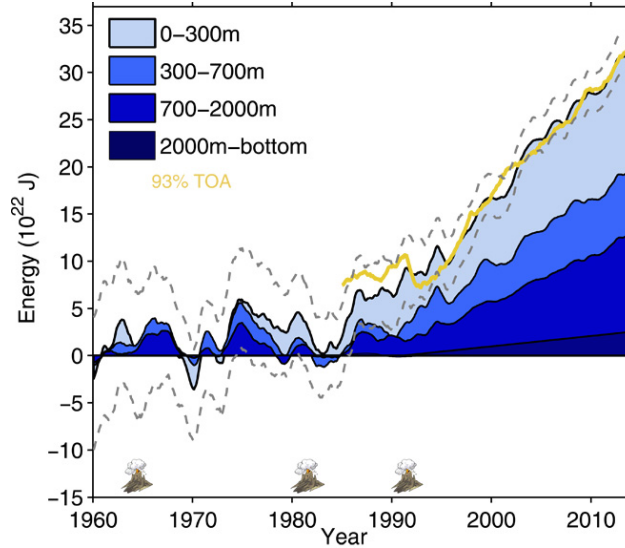


Figure VI.1 “Improved estimates of Sea heat content from 1960 to 2015”

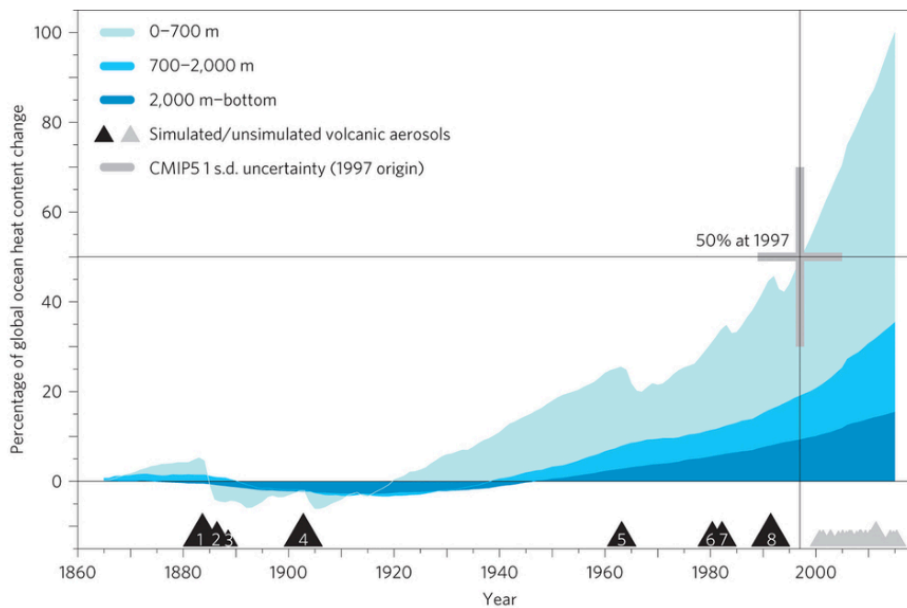


Figure VI.2 “Rate of heat storage has increased, with significant storage in deep ocean”

The two figures show a remarkable discrepancy. In figure VI.1 hardly any increase has been measured in the year 1960, where figure VI.2 presents a significant increase. Given the fact that the global warming started about 150 years ago, figure VI.2 gives a more reliable impression. However it only shows relative numbers.

Given the fact that all relevant variables in the global warming process up to this moment can be well represented as exponential functions, all with the time constant of 61 years, such a curve has been chosen to fit the increased heat energy between 1870 and 2015, *assuming* that the absolute value in 2015 in figure VI.1 is correct. The result *in first instance* is: $\Delta E_s(t) = -3.3 \cdot 10^{22} + 1.6 \cdot 10^9 \cdot \exp(t/61)$ Joule.

In order to check this assumption Table VI.1 has been calculated. This table shows the results for each layer in the year 2015, deduced from figure VI.1. The variable ΔV is the increased volume, only as a result of the expansion of the water, so $\Delta V = \Delta \text{temp (K)} \cdot \text{volume} \cdot \text{volume expansion coefficient of water (0.00021)} \text{ m}^3$. The variable $\Delta \text{height (cm)}$ is the resulting level rise, calculated as $100 \cdot \Delta V / \text{total surface of the Sea (3.6} \cdot 10^{14} \text{ m}^2)$. The total of Δtemp is the temperature increase *at the surface* of the Sea in 2015.

layer (m)	thickness (m)	volume (m ³)	$\Delta \text{energy (J)}$	$\Delta \text{temp. (mK)}$	$\Delta V \text{ (m}^3\text{)}$	$\Delta \text{height (cm)}$
0-300	300	$1.1 \cdot 10^{17}$	$1.3 \cdot 10^{23}$	303	$6.8 \cdot 10^{12}$	1,9
300-700	400	$1.4 \cdot 10^{17}$	$7.0 \cdot 10^{22}$	123	$3.7 \cdot 10^{12}$	1,0
700-2000	1300	$4.6 \cdot 10^{17}$	$1.0 \cdot 10^{23}$	54	$5.3 \cdot 10^{12}$	1,5
2000-3700	1700	$6.1 \cdot 10^{17}$	$2.0 \cdot 10^{22}$	8	$1.1 \cdot 10^{12}$	0,3
totals	3700	$1.3 \cdot 10^{18}$	$3.2 \cdot 10^{23}$	488	$1.7 \cdot 10^{13}$	4,7

Table VI.1 deduced from figure VI.1 for the year 2015

The remarkable result is that the temperature increase of 488 mK is half the measured temperature increase of the atmosphere in the year 2015. This observation leads to only one conclusion: the presented energy increase in all the layers are a factor 2 to low. Seemingly this check has not been carried out before presenting the results as shown in the figures above. The *final* result regarding the mathematical expression for $\Delta E_S(t)$ during the period 1870-2015 thus is:

$$\Delta E_S(t) = -6.6 \cdot 10^{22} + 3.2 \cdot 10^9 \cdot \exp(t/61) \text{ J} \quad (5)$$

The heat content of the Sea is measured by measuring the temperature in various places in the Sea as function of depth. The crucial question thus is how reliable these temperature measurements have been. Measuring the temperature at great depths requires very special and very accurately calibrated equipment. This consideration also shows that the smaller the temperature rise, not only as a function of depth, but especially in earlier years, the worse the relative accuracy must have been.

The calculation of the temperature increase in Table VI.1 is a rather rough one, given the fact that in reality most likely this temperature change, as function of depth, will much more look like an exponential function, with a yet unknown depth-constant c_d , as presented in: $\Delta T(d) = \Delta T_{\text{atm}} \cdot \exp(-d/c_d)$.

The expression: Specific heat capacity of water (C_h) \cdot Sea surface (S_s) $\cdot \int_0^\infty \Delta T(d) \cdot \delta d$ represents the total increase of heat energy of the Sea, given ΔT_{atm} . The boundary ∞ has to be read as the bottom of the Sea. The product $S_s \cdot \delta d$ is the value of the volume of the layer of water with thickness δd . The variable ΔT_{atm} is 1 K in 2015. The specific heat capacity of water equals $\sim 4 \cdot 10^6 \text{ J/m}^3/\text{K}$ and $S_s = 3.6 \cdot 10^{14} \text{ m}^2$. The equation to be investigated thus is: $\Delta E_{\text{total}} = 4 \cdot 10^6 \cdot 3.6 \cdot 10^{14} \cdot c_d \text{ J}$. Given the fact that this total heat energy has been corrected by a factor 2 to $6.4 \cdot 10^{23} \text{ J}$ in the year 2015, c_d is 444 m.

This approach shows that the transformation of the measured temperature increase as function of depth to finally the energy increase of the Sea as function of time, in the first place requires that the absolute temperature measurements are used to calculate c_d , of course as mean value over many places in the Sea. With this value the energy increase directly follows from $\Delta E_{\text{total}} = 4 \cdot 10^6 \cdot 3.6 \cdot 10^{14} \cdot c_d \text{ J}$.

The calculation presented above also offers the possibility to calculate the expansion of the Sea, in terms of its level rise, as a result of the increase of its temperature: $\Delta h = c_e \cdot \int_0^\infty \Delta T(d) \cdot \delta d = \Delta T_{\text{atm}} \cdot c_e \cdot c_d$, with c_e the volumetric expansion coefficient of water (0.00021 K^{-1}). For $\Delta T_{\text{atm}} = 1 \text{ K}$, $\Delta h = 9.3 \text{ cm}$.

Given the value of the total Δheight in Table VI.1 and the applied correction by a factor 2 to the measured/calculated heat energy of the Sea in the references [VI.1] and [VI.2], the outcome $\Delta h = 9.3 \text{ cm}$ creates confidence in the applied philosophy and calculations above.

This outcome will be used in chapter X: "Global Mean Sea Level until 2100".

VII Why the Greenhouse Model is untenable

VII.1 Introduction

In this chapter it will be proven in 6 sections why the Greenhouse Model is untenable. These sections are:

- VII.2 Principle of the GHM
- VII.3 A closer look at spectra
- VII.4 A closer look at the heat fluxes of the GHM
- VII.5 The heating of the Sea in the GHM
- VII.6 The GHM applied on Mars and Venus
- VII.7 The Reverse Greenhouse Effect

The Reverse Greenhouse Effect expresses that the higher the temperature of the atmosphere is the more it absorbs CO₂ at the cost of the absorption by Earth's surface, given a certain amount of emission. If the Reverse and the normal Greenhouse Effect would exist together, a positive feedback loop would have been created, leading to an explosive process.

VII.2 Principle of the GHM

It is beyond dispute that half of the Earth is heated during the day and that, at the same time, the other half gives off the previously absorbed heat during the night. That release is eventually done to the universe through radiation. According to the GHM, cooling is more impeded by the atmosphere the more it contains greenhouse gases. The defence that these greenhouse gases should therefore hinder the much stronger incoming solar radiation too and thus cool the Earth is refuted by the following alleged reasoning put forward by the GHM supporters.

The incoming radiation has a shorter wavelength than the cooling one. According to the GHM, this short-wave radiation is not blocked by the greenhouse gases, while the long-wave radiation is. The spectrum of the solar radiation is maximum at a wavelength of ~ 600 nm. According to the GHM, the spectrum of the cooling radiation lies at a wavelength of ~ 20000 nm.

N.B. It is not mentioned that the cooling starts primarily with convection through the atmosphere, to eventually be completed as radiation from the exosphere.

VII.3 A closer look at spectra

Originally the idea, based on the above-described principle of the GHM, was that a thorough theoretical investigation of the spectrum of the radiation during cooling is essential. After this investigation was completed, it appeared to play no role. The result of the investigation is considered noteworthy. In brief:

The cooling hemisphere of the Earth will be regarded as a black radiator, with a temperature at the surface of 525 K (250 °C). The note on that surface is that the associated so-called exosphere is so thin that it borders on vacuum. By definition vacuum has no temperature. But only 1 molecule in any volume does! The temperature of that exosphere is very high indeed. The maximum of the spectrum of its radiation is, at a temperature of 250 °C, at a wavelength of ~ 10000 nm. So not at the 20000 nm, as alleged by the GHM. The temperature of a black radiator with the maximum at a wavelength of 20000 nm is -20 °C!

VII.4 A closer look at the heat fluxes of the GHM

“Heat flux” stands for: “heat power per surface unit” and is therefore expressed in W/m².

The GHM focuses on heat fluxes, mainly in the form of radiation, which are intended to indicate the heating and cooling of the Earth. All this is done by means of figure VII.1, copied from reference [VII.1], intended to provide insight. The yellow fluxes represent the heating and the red, upward, the cooling. The downward directed red ones, referred to as radiation from greenhouse gases, are thought to determine the heating of both the atmosphere and the Sea. The “net absorbed” flux is claimed to be 0.6 W/m² in 2010.

However, in no way whatsoever it can be found that this alleged net absorbed flux should be 0.6 W/m^2 . Further study of reference [VII.1] also offers no guidance. It is therefore unbelievable that this small difference could have been derived from the much larger fluxes, with an accuracy that also suggests to be significant smaller than 0.1 W/m^2 .

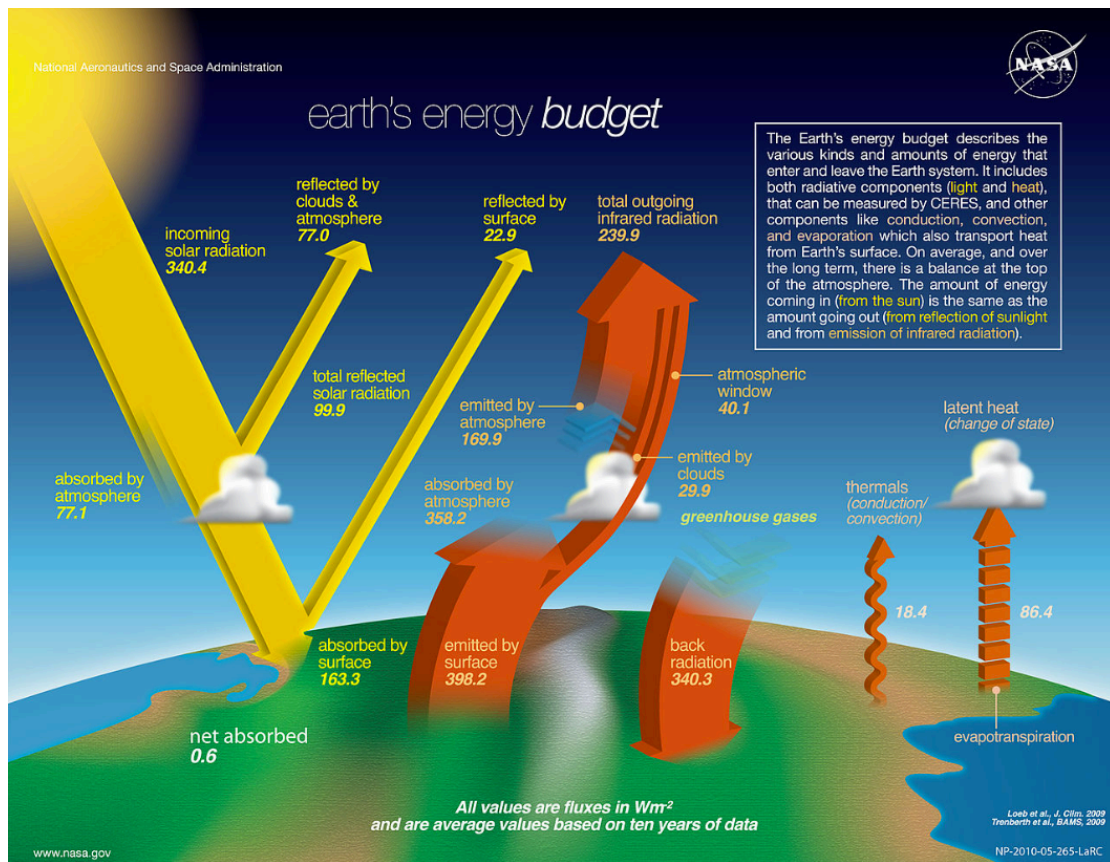


Figure VII.1

Reference [VII.1] reports under the chapter “Climate Forcings and Global Warming”:

“The absorption of outgoing thermal infrared by carbon dioxide means that the Earth is still absorbing about 70 percent of the incoming solar energy, but an equivalent amount of heat is not emitted again. The exact amount of energy imbalance is very difficult to measure, but turns out to be slightly more than 0.8 watts per square meter. The imbalance is derived from a combination of measurements, including... .. observations of sea level rise and warming.”

In the next section it is made plausible that the last sentence should almost certainly have read: The imbalance is *only* deduced from the measured increased temperature of the Sea, transformed to warmth.

Reference [VII.2] is also particularly unconvincing given the fact that measurements of “thermal infrared radiation emitted to space” cannot distinguish between radiation as a result of the alleged greenhouse effect and radiation from heat generated by human energy consumption.

VII.5 The heating of the Sea in the GHM

According to the GHM the Sea is heated top down to great depth, gradually decreasing to zero, while simultaneously the atmosphere is heated too. In the previous section it is shown that the alleged related “net absorbed” heat flux/power density is presented as 0.6 W/m^2 in 2010, “based on the average values over the past 10 years”. Such a calculation cannot lead to a power density in exactly the year 2010. It would result in the mean value of the power densities over these 10 years and thus nothing tell about the temperature increase of the Sea in exactly 2010.

Given the investigations in chapter VI such a power density can be calculated now by differentiating equation (5): $\Delta E_s(t) = -6.6 \cdot 10^{22} + 3.2 \cdot 10^9 \cdot \exp(t/61)$, leading to $P_s(t) = 3.2 \cdot 10^9 / 61 \cdot \exp(t/61)$ J/year and after dividing by the number of seconds per year ($3.15 \cdot 10^7$) to $1.65 \cdot \exp(t/61)$ Watt.

After dividing this power by the Sea surface of $3.6 \cdot 10^{14}$ m² the result is a power density of $PD_s(t)$ equal to: $4.6 \cdot 10^{-15} \cdot \exp(t/61)$ W/m². So in the year 2010 the variable $PD_s(2010) = 0.9$ W/m².

It thus has to be concluded that the following two mistakes have been made in the presentation of the power density in 2010 in figure VII.1. In the first place not the increased heat energy in this year has been taken, but the mean value over the past 10 years. In the second place it has not been shown which information about increased energy levels in the Sea has been used. And if the values of figure VI.1 would have been used, the outcome would have been, right at the start already, a factor 2 too low, as has been proven in chapter VI.

The top down heating of the Sea to a great depth should be considered impossible. Convection is out of the question because a thin layer of heated water keeps floating at the surface. And conduction is not possible as can be proven with the associated physical law $\Delta T = R \cdot \Phi$ with:

Φ	the applicable heat flux	W/m ²
R	the thermal resistance	K/(W/m ²)
ΔT	the temperature difference	K

The thermal resistance, to be considered, of the layer of water with thickness d is determined by $R=d/\lambda$, with λ the specific thermal conductivity of water: 0.6 W/(m·K). The thermal resistance R of a layer of water of 3600 m is therefore $3600/0.6 = 6000$ K/(W/m²). Applying the heat flux 0.6 W/m² of the GHM to this, leads to a ΔT of 3600 K. This result has to be interpreted as the impossibility of allowing such a heat flux to flow through such a layer of water by means of conduction.

The counter argument put forward by Ocean Specialists is that the Sea does not stand still, meaning that it has a three dimensional circulation that takes heat from the surface into the subsurface layers, for example caused by: storms mixing the upper 100 m, large-scale winds that drive Sea currents filling Sea basins to depths greater than 1000 m, equatorial waters flowing in the direction of the poles and tidal currents. This phenomenon has got the name “thermohaline circulation”.

It will be shown in section VIII.5 that most likely that the so-called geothermal heat flux, instead of the alleged heat flux resulting from the GHM, is responsible for the heating of the Sea. Bottom up! Since the heating starts at great depths and the water thus heated wants to rise, it does not require much imagination to consider this process as the cause of the thermohaline circulation, instead of a means of explaining the heating of the Sea top down.

VII.6 The GHM applied on Mars and Venus

The surface temperature on Mars is -63 °C, its atmosphere has a pressure of 0.01 atm. These values at Venus are 500 °C, respectively 100 atm. The atmosphere of both planets consists of 96% CO₂.

It is generally believed that, due to the CO₂ in the atmosphere, Earth’s temperature increase is expressed by $\Delta T_E = 0.007 \cdot \Delta CO_2$ (ppm). See Chapter V. To convert this expression to the situation on Mars the gradient 0.007 must first be reduced by 2.3 due to the larger distance from the Sun. Secondly be multiplied by 100, due to the fact that the heat capacity of Mars’ atmosphere is 100 times smaller.

At a CO₂ concentration of almost 1 million ppm, a temperature increase of 300 thousand °C should thus be observed on Mars. Applying this method to Venus results in a temperature increase of 135°C. The result for Mars is absurd enough to reject such a transformation, or to reject the Greenhouse Model.

What has been overlooked is the role of the geothermal flux on the planets, which originates in their core. As on Earth, these cores radiate their energy into space through the atmosphere, which on Mars means that this radiation is hardly hindered by its atmosphere, while on Venus the isolation of this layer is about 10 thousand times higher. This phenomenon simply explains the observed large temperature difference at the surfaces of these planets and makes the just mentioned choice easy: the GHM has to be rejected.

VII.7 The Reverse Greenhouse Effect

A detailed study of the CO₂ concentration in the atmosphere as a result of the CO₂ emission eventually learns that the CO₂ concentration increases with the temperature of the atmosphere. This phenomenon has been given the name Reverse Greenhouse Effect. This effect would have an disastrous effect on the global warming, because together with the Greenhouse effect it would create a process with a positive feedback, leading to an explosive increase of the temperature of the atmosphere.

VII.7.1 CO₂ emission factor in terms of Gigaton/consumed energy

CO₂ emissions, as a result of the combustion of fossil fuels, are for example expressed in terms of the number of tons of CO₂ per released amount of energy in TeraJoule. This emission factor depends on the type of fossil fuel. Reference [VII.3] shows the following CO₂ emission factors, together with the here added transformation factor: 'Gigaton CO₂/TWyear'.

	ton CO ₂ /TeraJ	Gt CO ₂ /TWyear
gas	55	1,7
oil	74	2,3
coal	100	3,2

Table VII.1

The relative distribution of the consumed energy in the years 2010, 1910 and 1810 of these fuels is shown in table VII.2 on the left side. The emission factor of biofuel/biomass is taken the same as of coal. The contributions of Nuclear and Hydro-elect energies (both 5%) to the CO₂ emissions are left away. The column in the middle shows the related emission factor from Table VII.1. The right side of Table VII.2 shows the left side, after multiplication with the middle column.

	emission factor in Gt/TeraWatt-year						
	2010	1910	1810	X	2010	1910	1810
Gas	0,20	0	0	1,7	0,4	0,0	0,0
Oil	0,31	0	0	2,3	0,7	0,0	0,0
Coal+Biomass	0,39	1	1	3,2	1,2	3,2	3,2
				sum	2,3	3,2	3,2

Table VII.2

In the next section this 'sum', being the weighed average emission factor, will be applied in the years 1850 – 2050 in steps of 20 year. The values for the years since 1910 are found by linear interpolation between the values at 1910 and 2010. The values for 2030 and 2050 are taken the same as for 2010 is.

year	1850	1870	1890	1910	1930	1950	1970	1990	2010	2030	2050
emission factor	3,2	3,2	3,2	3,2	3,0	2,8	2,7	2,5	2,3	2,3	2,3

Table VII.3 Emission factor in Gt/TWyear

VII.7.2 CO₂ concentration expressed in Gigaton

The CO₂ concentration in the atmosphere is normally expressed in ppm, that is to say, the amount of CO₂ in relation to the amount of molecules in the atmosphere, both expressed in mol.

The total mass of air in the atmosphere is $5.3 \cdot 10^{18}$ kg. Given the definition of ppm, this mass has to be converted to the unit mol, defined as the mass of N_A atoms/molecules of that substance. N_A is the number/constant of Avogadro ($6 \cdot 10^{23}$ mol⁻¹). The mean molar mass of air is 29 kg/kmol, so the amount of 'mean' air molecules in the atmosphere is $5.3 \cdot 10^{18} / 29 = 1.8 \cdot 10^{17}$ kmol.

The worldwide mean concentration of 400 ppm CO₂ in the atmosphere in the year 2018 thus represents $400 \cdot 10^{-6} \cdot 1.8 \cdot 10^{17} = 7.3 \cdot 10^{13}$ kmol CO₂. The molar mass of CO₂ is 44 kg/kmol, so the mass of 400 ppm CO₂ in the atmosphere is $44 \cdot 7.3 \cdot 10^{13} = 3.2 \cdot 10^{15}$ kg = 3200 Gigaton (Gt). The conversion from ppm CO₂ to *absorbed* Gt CO₂ in the atmosphere thus is 3200/400 = 8 Gt/ppm.

This factor has been used calculating ΔCO_{2aA} from ΔCO_{2aR} in table VII.4

year	atmospheric absorption			emission			results	
	CO _{2a} (ppm)	ΔCO_{2aR} (ppm/year)	ΔCO_{2aA} (Gt/year)	Power (TW)	E factor (Gt/TWyear)	CO _{2e} (Gt/year)	CO _{2s} (Gt/year)	$\Delta\text{CO}_{2aA}/\text{CO}_{2e}$ (%)
1850	269	0,15	1,2	1,2	3,2	4,0	2,7	31
1870	273	0,22	1,7	1,7	3,2	5,5	3,8	31
1890	278	0,30	2,4	2,4	3,2	7,7	5,3	31
1910	285	0,4	3,3	3,3	3,2	10,6	7,3	31
1930	295	0,6	4,6	4,6	3,0	13,9	9,3	33
1950	308	0,8	6,4	6,4	2,8	18,2	12	35
1970	327	1,1	8,9	8,9	2,7	23,7	15	37
1990	353	1,5	12	12	2,5	31	18	40
2010	390	2,1	17	17	2,3	39	22	43
2030	440	3,0	24	24	2,3	55	31	43
2050	510	4,1	33	33	2,3	76	43	43

Table VII.4

CO _{2a}	relative CO ₂ concentration in the atmosphere	[ppm]
ΔCO_{2aR}	relative increase of CO ₂ in the atmosphere	[ppm/year]
ΔCO_{2aA}	absolute increase of CO ₂ in the atmosphere (=8· ΔCO_{2aR})	[Gt/year]
Power	applied power by mankind (*)	[TW]
E factor	emission factor for CO ₂ , as shown in table VII.3	[Gt/TWyear]
CO _{2e}	emitted CO ₂ per year (E factor · Power)	[Gt/year]
CO _{2s}	absorbed CO ₂ by Earth's surface per year (CO _{2e} - ΔCO_{2aA})	[Gt/year]
$\Delta\text{CO}_{2aA}/\text{CO}_{2e}$	relative (to CO _{2e}) increase of CO ₂ absorbed by atmosphere	[%]

(*) By applying power (in terms of TW) instead of energy (in terms of TWyear), the multiplication of this power by the emission factor, expressed in Gt/TWyear, results in the CO_{2e} in Gt/year.

Check of the column ' ΔCO_{2aA} '.

Digital integration of the column ' ΔCO_{2aA} ' by taking 20 times the value of each year, up to and including the year 1990, plus 8 times the value of 2010 in order to find the result for the period 1850 - 2018, shows 953 Gigaton. This result has to be compared with the difference between the CO₂ concentration in 2018 (400 ppm) and in 1850, multiplied by 8 Gt/ppm. That outcome is 1048 Gigaton. The 10% difference is caused by the large integration step of 20 years.

Remark:

In first instance the columns ' ΔCO_{2aA} ' and 'Power' show surprisingly exactly the same numbers. The background is as follows. ' ΔCO_{2aA} ' is calculated as the derivative of $\text{CO}_2(t) = 259 + 6.4 \cdot 10^{-13} \cdot \exp(t/61)$, shown as equation (1) in chapter I, times 8 Gt/ppm, resulting in: $8.4 \cdot 10^{-14} \cdot \exp(t/61)$ ppm/year.

The variable 'Power' is fitted by $P_G(t) = 8.4 \cdot 10^{-14} \cdot \exp(t/61)$ TW, shown as equation (4) in chapter IV.

The importance of the variable ' $\Delta\text{CO}_{2aA}/\text{CO}_{2e}$ ' will be considered in the next section

VII.7.3 Short term evidence for the existence of the Reverse Greenhouse effect

Table VII.4 in the previous section shows that most of the CO₂ emission is absorbed by Earth’s surface. It also shows that the absorption increases with time from roughly a 30–70 to a 40–60% distribution. During that same period the temperature of the atmosphere increased 1°C.

Given this phenomenon the following *hypothesis* is posited: the measured increase of the CO₂ concentration in the atmosphere is *only* caused by the increase of its temperature. A Reverse Greenhouse Effect.

If this hypothesis would be valid then the gradient of the growth of the CO₂ concentration in the atmosphere, as function of atmosphere’s temperature, would be 145 ppm/°C, as shown in chapter V.

In chapter II it has been found that the temperature of the atmosphere changes, on top of the long-term-trend, with $-0.1 \cdot \sin\{\omega(t - 2012)\}$ (°C), in which ω represents a period of 64 years. Chapter I shows the CO₂ measurements during the period 1958-2018. These 60 years form a just long enough period to investigate the relation between atmosphere’s CO₂ concentration and temperature in more detail.

Figure VII.2 shows the measured CO₂ minus the exponential fitted curve +0.5, indicated as “measured”. The “+0.5” is applied in order to make the curve symmetrical around zero, just like the, to investigate, sinusoidal CO₂ curve is. This curve has been drawn with two amplitudes, indicated as “theoretical CO₂ 1.5 ppm” resp. as “theoretical CO₂ 1.0 ppm”. Comparison with the measured curves leads to the conclusion that the hypothesis has to be rejected, because the amplitude should have been 0.1 times 145, say 15 ppm. But still it clearly shows an influence of atmosphere’s temperature on its CO₂ concentration.

A partially Reversed Greenhouse Effect has been demonstrated, with a gradient of 10 to 15 ppm/°C.

The word ‘partially’ has to be understood as: only about 10% of the total increase of the atmospheric CO₂ concentration is caused by the atmospheric temperature increase. The other 90% is caused by emission.

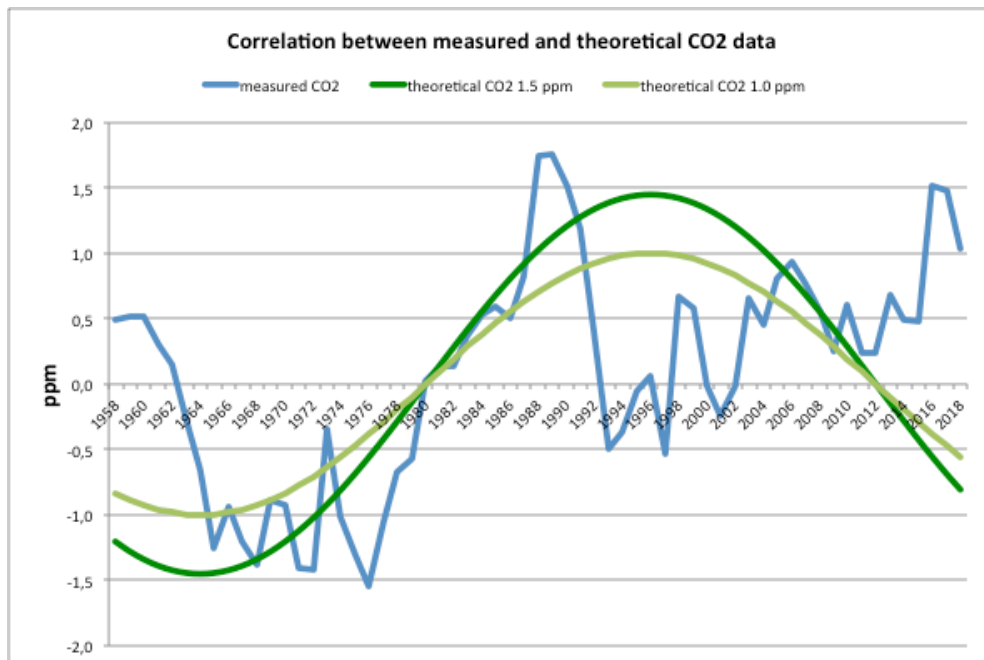


Figure VII.2

Another way of presenting the correlation between “measured CO₂” and “theoretical CO₂” is to fit a high order polynomial curve to the differences between the measured CO₂ data and the exponential fitting of this data, as shown in chapter I. Taking a 8th order fitting of these deviations the result is as shown in figure VII.3. The resemblance is fundamentally the same as shown in figure VII.2.

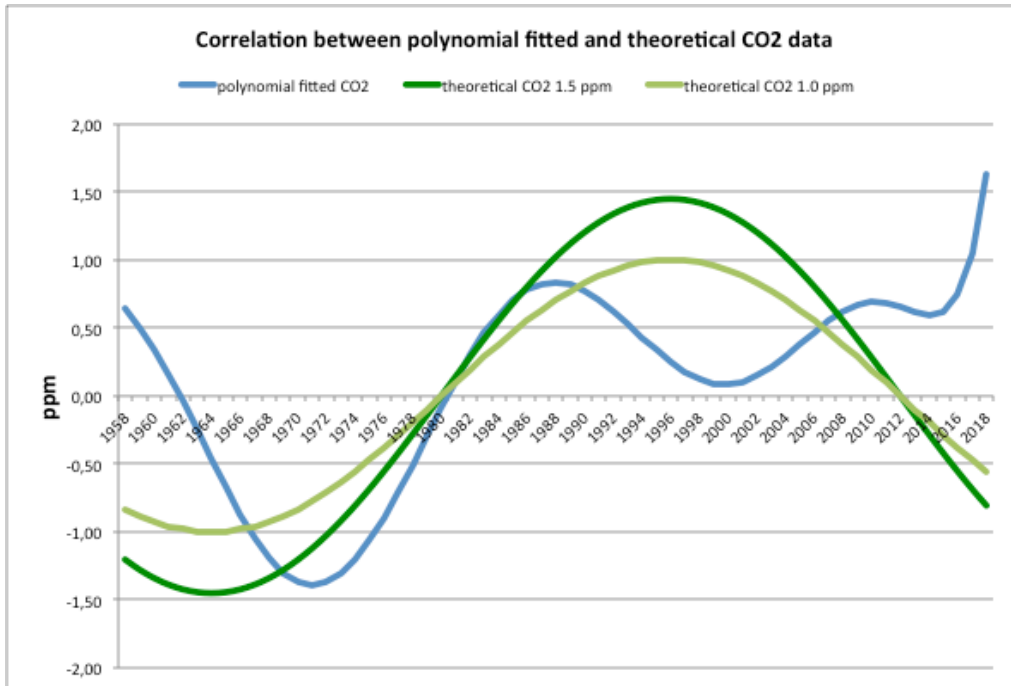


Figure VII.3

Figure VII.4 shows that there is in the same period of 60 years a rather high resemblance between the patterns of the *random* CO₂ and *random* temperature deviations. To investigate this, the derivative in each year has been calculated for both variables. The quotient of these derivatives has been calculated in case they are both positive and in case they are both negative. This turned out to happen in 32 of the 55 years. Such a result is from a statistical point of view not convincing. But their mean value is ~ 10 ppm/ $^{\circ}$ C, showing a remarkable good agreement with the range 10 - 15 ppm/ $^{\circ}$ C, found in the sinusoidal curve.

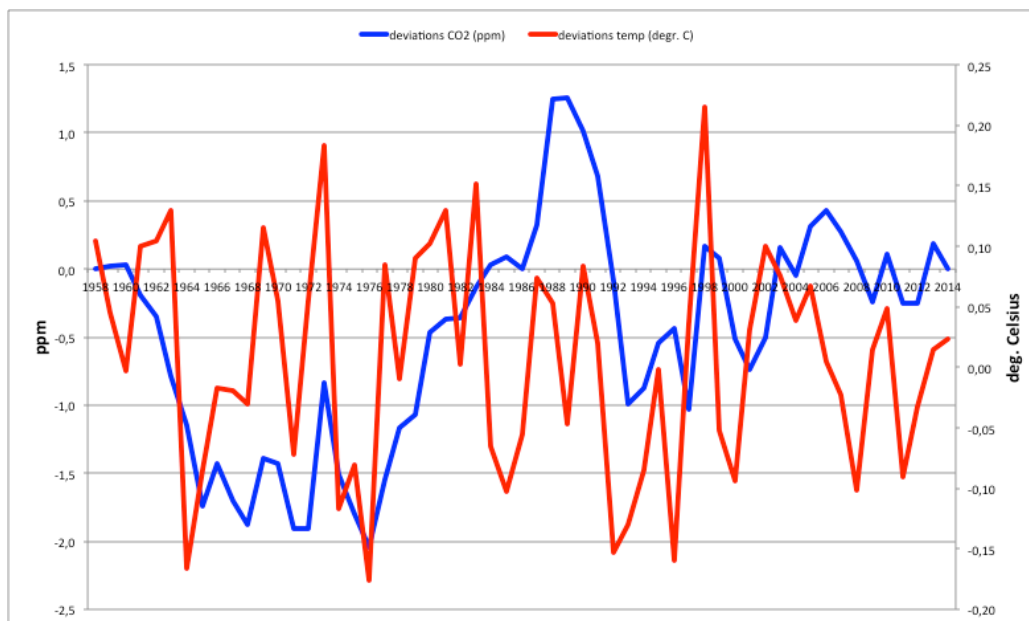


Figure VII.4 Yearly random deviations of global temperature and atmospheric CO₂ concentration

VII.7.4 Long term evidence for the existence of the Reverse Greenhouse effect

Figure VII.5 shows very long term historical relations between CO₂ and global temperature. This figure has been deduced from the original article, ref. [VII.4]*. The abstract sounds:

“The recent completion of drilling at Vostok station in East Antarctica has allowed the extension of the ice record of atmospheric composition and climate to the past four glacial–interglacial cycles. The succession of changes through each climate cycle and termination was similar, and atmospheric and climate properties oscillated between stable bounds. Interglacial periods differed in temporal evolution and duration. Atmospheric concentrations of carbon dioxide and methane correlate well with Antarctic air-temperature throughout the record. Present-day atmospheric burdens of these two important greenhouse gases seem to have been unprecedented during the past 420,000 years.”

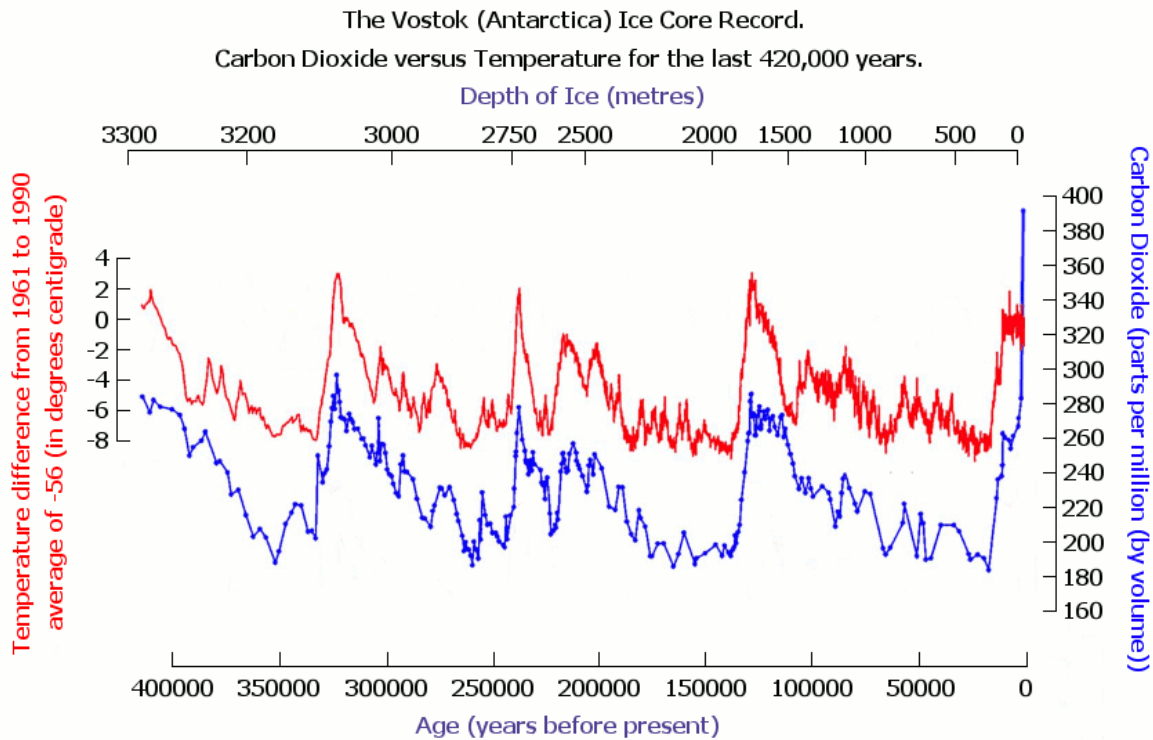


Figure VII.5 420000 years of global temperature and atmospheric CO₂ concentration

From the point of view of the Reverse Greenhouse Effect it is interesting to deduce, just like it is done in figure VII.4, the ratio: $\Delta\text{CO}_2(t)/\Delta T(t)$. Given the uniformity between the two curves in Figure VII.5, only one sample is already representative for the whole period. This sample is taken at the steep change in the middle of the graph, where $\Delta\text{CO}_2/\Delta T \sim 80/8 = 10 \text{ ppm}/^\circ\text{C}$, being in remarkable good agreement with the gradient 10-15 ppm/^oC of the Reverse Greenhouse Effect and thus not at all in agreement with the greenhouse effect. So the temperature variations over the past 420000 years have not been caused by CO₂ variations, but vice versa. What has been proven with the Vostok study is the validity of the Reverse Greenhouse Effect, instead of the Greenhouse Effect.

Around the year 0 (present time) a very long and steep curve upwards of the CO₂ concentration is drawn, in conformity with reality, however without a clearly visible increase of the temperature. That confirms the presentation of the present process, indeed being very different from the historical processes.

The consequence of the existence of the Reverse Greenhouse Effect is that the Greenhouse Model must be declared non-existent, because if they would exist together, an increase in atmospheric temperature would cause an increase in the atmospheric CO₂ concentration, which in turn would lead to an increase in atmospheric temperature. Definitely an explosive process.

*The figure exactly as shown here seems not to be available anymore on Internet after about 5 years!

VIII Living Room Model

VIII.1 Introduction

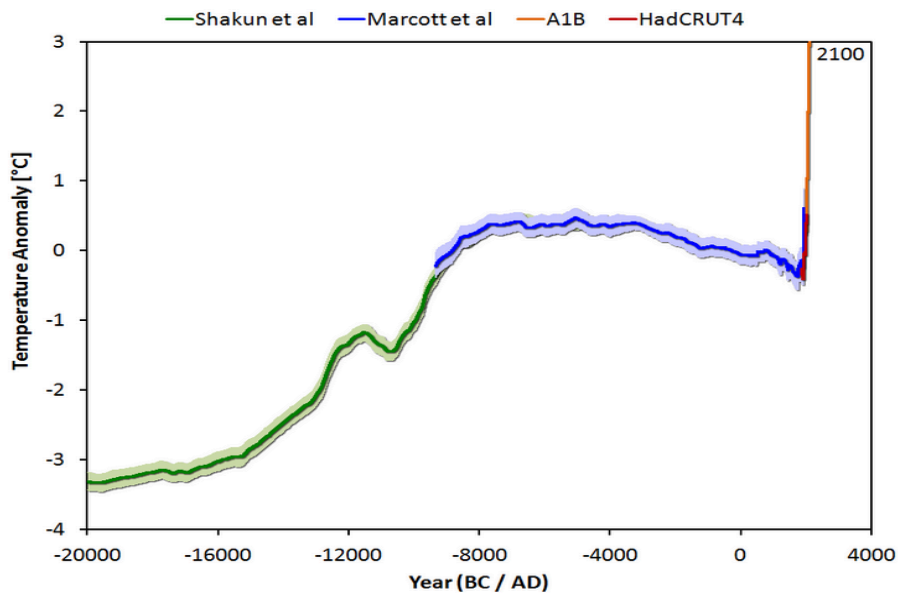
Imagine a living room occupied by a lot of people being very busy with whatever. The more people and / or the more hustle and bustle, the higher the temperature in that living room rises, assuming no external influences. This situation perfectly resembles the Earth's atmosphere in which many people consume a lot of energy of any kind.

The thermodynamic law of conservation of energy forces us to conclude that all energy consumed worldwide, of whatever nature, such as solar, wind and nuclear energy, is eventually converted into heat. Also when basic energy is converted into kinetic energy, such as with propulsion. This kinetic energy is inevitably converted into heat by friction with the medium in and on which the propulsion takes place, and by the friction in the machine itself. If the propulsion also results in an increase in the potential energy of the vehicle, as in the case of an airplane, or a car driving up a mountain, this potential energy is still converted into heat as soon as the vehicle returns to its original height.

By converting solar energy into electrical energy, that part is eventually transformed into thermal energy in the atmosphere, fully equivalent to, for example, the heat generated by fossil combustion. It could be argued that if this part had not been converted into electrical energy, it would still have heated the Earth's surface and the atmosphere. But history has proven for thousands of years that solar heating did not raise the temperature of the atmosphere higher than the level it was 200 years ago. It must therefore be seriously taken into account that generating electrical energy from solar energy will not contribute to the reduction of the warming of the atmosphere.

VIII.2 Heat balance of the atmosphere

Apparently there has been a balance between absorbed and released heat by the atmosphere for many centuries, but this balance has been severely disrupted for about 200 years, as shown in figure VIII.1. This disturbance has an increase in the global temperature with a time-dependent gradient as shown in Table VIII.1. These values can be calculated by taking the derivative to time of (2) in chapter II.



year	mK/year
1850	1,1
1875	1,6
1900	2,4
1925	3,7
1950	5,5
1975	8,3
2000	12,5
2005	13,6
2010	14,7
2020	17,4
2100	64,5

Figure VIII.1: Global temperature since the year -20000

Table VIII.1 Gradient global temperature

VIII.3 The heating of the atmosphere in the LRM

In order to calculate the temperature increase of the atmosphere by *direct* heating, it is necessary to know its heat capacity. The heat capacity of the atmosphere, expressed in J/K, determines how much the atmosphere rises in temperature, given the *net* heat supplied to it. Here "net" is defined as the difference between the supplied and released heat. In Appendix 2 it has been calculated by two methods that this heat capacity is $5 \cdot 10^{21}$ J/K.

In as well the GHM as the LRM the (alleged) supplied heat is well defined. It is not known which part of it is released, in order to calculate the net supplied heat. But the actually measured temperature rise as function of time is known and can be expressed mathematically by equation (2).

The following equation applies in both models:

$$\text{"Atmospheric heat capacity [J/K]" times "atmospheric temperature increase during a year [K/year]" = "net heat energy absorbed by the atmosphere during that year [J/year]"}$$

The dimension [J/year] is equivalent to the dimension [W], so the last mentioned variable in the equation above can also be presented as: "net average heat power applied during that year", expressed in W. The atmospheric heat capacity can also be written in the dimension W/(K/s). Table VIII.1 shows that the atmospheric temperature gradient in 2010 was $14.7 \text{ mK/year} = 0.0147/3.1536 \cdot 10^7 = 4.7 \cdot 10^{-10} \text{ K/s}$. So in the year 2010 a net heat power of: 'Atmospheric heat capacity' times 'atmospheric temperature gradient', being: $5 \cdot 10^{21} \cdot 4.7 \cdot 10^{-10} = 2.4 \text{ TW}$ is sufficient to achieve that gradient in 2010.

Equation (4) shows that the globally applied power in 2010 is $8.4 \cdot 10^{-14} \cdot \exp(2010/61) = 17.2 \text{ TW}$. The required net power, to heat the atmosphere as has been measured, thus is only 14% of this globally generated power. In other words and in terms of energy: by far the largest part (86%) of the gross heat energy, generated by the LRM in 2010, is radiated to space. The remaining part is sufficient to increase the temperature of the atmosphere as has been measured during that year.

The generated gross power of the LRM can be expressed in terms of (mean) global gross power density, by dividing this power by Earth's surface ($5.1 \cdot 10^{14} \text{ m}^2$), resulting in 0.034 W/m^2 . This value compared to the value of the GHM (0.6 W/m^2 , to be corrected to 0.9 W/m^2) shows an extremely large difference of almost a factor 30. The cause is that the GHM-value, in terms of radiation, is *created* instead of actually *measured* in order to explain the heating of the Sea.

VIII.4 LRM heating since 1810

The derivative of the *actually measured* temperature gradient equals the derivative of equation (2), being: $7.2 \cdot 10^{-14} \cdot \exp(t/61) \text{ mK/year}$.

Taking 14% of the globally applied power, equation (4) results in: $0.14 \cdot 8.4 \cdot 10^{-14} \cdot \exp(t/61) \text{ TW}$.

This result in Watt, divided by the heat capacity of the atmosphere and multiplied by the ratio "sec/year", results in $7.4 \cdot 10^{-14} \cdot \exp(t/61)$. The small deviation from the *measured* $7.2 \cdot 10^{-14} \cdot \exp(t/61) \text{ mK/year}$ is eliminated when the heat capacity of the atmosphere is taken $5.1 \cdot 10^{21}$ instead of $5.0 \cdot 10^{21} \text{ J/K}$!

Qualifying this expression as the *calculated* temperature gradient as function of the world wide applied power, it has been proven that this calculated yearly increase of the global temperature during the past 200 years, perfectly matches the *measured* yearly increase of the global temperature. And thus can be predicted too on this basis!

VIII.5 The heating of the Sea in the LRM

In view of the findings in section VII.5 “The heating of the Sea in the GHM”, such a heating can only take place bottom up and by means of convection.

The application of a heat pump with a so-called horizontal ground exchanger (at a depth of 2 meters) teaches that a continuous heat flux of 50 W/m² can be generated. But then the temperature at that depth drops from +10 °C to -5 °C. At such a place heat is extracted from Earth in a forced way. Incidentally, that temperature will return to its original value within a few hours after the heat abduction has been stopped. So most likely the *natural* geothermal heat flux is at least an order of magnitude lower than this *forced* heat flux of 50 W/m².

In section VII.5 it has been shown that the power density, forcing the increase of the heat content of the Sea, can mathematically be expressed as $PD_s(t) = 4.6 \cdot 10^{-15} \cdot \exp(t/61)$ W/m². This heat flux varies from 0 to 1 W/m² during the period 1870-2020, and is much lower than the mentioned *forced* geothermal heat flux of 50 W/m², so fully acceptable as possible source of the heating of the Sea. The unknown natural geothermal heat flux most likely has been constant during the past several thousands of years. The (exponentially) increasing heat flux, responsible for the heating of the Sea, has to be considered as that part of the natural geothermal heat flux that heats the Sea, while its remaining part is radiated into space. Just as it did until 1870 without adding heat energy to the Sea, because the temperature of the atmosphere hadn't risen yet.

In order to understand the influence of that geothermal heat flux on the temperature of the Sea, we consider a basically comparable situation: a river flowing into a sea. Mind the difference between sea and Sea! The level of that sea varies with the tide. The level of the river water in the estuary rises and falls without delay with the level of the sea. The further inland, the less remains in the river of that varying level in the estuary.

If we replace, in this reality, the height of that sea by the temperature of the atmosphere, then the temperature difference at the transition of the atmosphere and the Sea's surface is always zero, given the slow change in temperature of the atmosphere. Thus, as the long-term temperature of the atmosphere increases, the long-term temperature of the Sea at its surface increases by the same amount, through the supply of thermal energy in the form of geothermal heat flux. And for this reality also applies: the deeper into the Sea, the less remains of that increase in temperature at the surface.

The amount of heat in the Sea is $15 \cdot 10^{26}$ Joule, as follows from the parameters below:

specific heat capacity per m ³	$4.0 \cdot 10^6$	J/K/m ³
volume	$1.3 \cdot 10^{18}$	m ³
mean temperature	280	K

The increased amount of heat in the Sea over the past 150 years has been corrected to $64 \cdot 10^{22}$ Joule. In comparison to the total amount of heat in the Sea this is only about 0.4 ‰!

Summarized: The geothermal heat flux, that has existed for millions of years, once brought at some moment the Sea and the atmosphere to certain temperatures, equal to each other at the transition of both media. As mankind has raised the temperature of the atmosphere by 1 °C, the geothermal heat flux does adjust the temperature at the surface of the Sea to this increase, gradually decreasing to 0 at the bottom.

N.B.

Permafrost is of course in the same way affected by the geothermal heat as the Sea is heated by this phenomenon.

VIII.6 Hot Spots on Earth

Hot Spots are columns in the atmosphere where the temperature is significantly higher than the mean temperature of the atmosphere. The explanation for these thermal columns cannot be given by the GHM. After all, a column of increased CO₂ concentration would be spread over the rest of the atmosphere before that gas would be able to cause an increase in temperature exactly above the considered surface. Only a *continuous* heat flow, significantly higher than the globally mean value, can maintain such a local higher temperature. The force of that flow/flux is proportional to the applied power on the related area, divided by the surface of that area. No data has been found on the Internet about the amount of energy consumed per country per year. There are data of the Gross Domestic Product (GDP), expressed in US \$, per country per year. It is *assumed* that the higher the GDP of a country, the more energy is consumed. In order to transform 'GDP' to 'Watt' the globally GDP (GWP), i.e. the sum of the GDPs of all countries, has been divided by the globally applied power, as shown by (4): $P_G(t)=8.4 \cdot 10^{-14} \cdot \exp(t/61)$. According to reference [VIII.1], the GWP for the year 2015 is about 75000 billion ($75 \cdot 10^{12}$) \$. In that year the applied power was 19 TW. The requested conversion factor thus is 0.25 W/\$. Ref. [VIII.2] and [VIII.3] show, by country, their GDP in 2015, respectively their surface. These values have been converted to \$ resp. m².

The power density per country can now be calculated from: $GDP(\$)/surface(m^2) \cdot 0.25 W/\$$ in W/m². The results of the 10 countries with the highest resp. lowest values are shown in Table VIII.2 resp. VIII.3. The warming of the Netherlands is measured as twice as high as the rise of the global mean value. See reference [VIII.4]. Due to the influence of the surrounding atmosphere a factor 2 higher than the global mean value in 2015: $19 TW/5.1 \cdot 10^{14} = 0.037 W/m^2$ would not be enough of course. But still the value 4.5 is surprisingly high. Multiplying the power densities with the related surfaces and adding these results shows a worldwide applied power of $18 \cdot 10^{12} W$. The difference with the number $19 \cdot 10^{12} W$ is caused by the fact that about 20 of the 200 countries are not found in as well reference [VIII.2] as in [VIII.3].

Country	W/m ²	Country	W/m ²
Singapore	101	Guyana	0,0037
Bahrain	9,9	Namibia	0,0035
Malta	7,6	Mali	0,0026
San Marino	6,5	Chad	0,0021
Luxembourg	5,5	Mongolia	0,0019
Netherlands	4,5	Niger	0,0014
Switzerland	4,0	Mauritania	0,0012
Belgium	3,7	Zimbabwe	0,0009
Qatar	3,6	Kyrgyz Republic	0,0008
Korea	3,4	Suriname	0,0008
Israel	3,4	Central African Rep.	0,0006

Table VIII.2 Highest ranked countries

Table VIII.3 Lowest ranked countries

If only Earth's land (30% of the total surface) is chosen as the reference surface, as is effectively done in the above calculations, the related mean power density in 2015 would be 0.12 W/m².

The five countries: Nigeria, Estonia, Equatorial Guinea, Indonesia and Bulgaria show roughly this value. These countries are ranked around the position 70 in the list of 180.

The total power of the 17 countries below, in descending order, includes 80% of the worldwide applied power. The related mean power density is 0.2 W/m² and the total surface 0.4 times Earth's land surface.

These 17 countries are: United States, China, Japan, Germany, United Kingdom, France, India, Italy, Brazil, Canada, Korea, Russia, Australia, Spain, Mexico, Indonesia, Netherlands.

IX Monthly global temperature and CO₂ anomalies

Monthly averaged records of the global temperature and of the CO₂ concentration in the atmosphere show both a surprisingly yearly periodic anomaly.

IX.1 Monthly temperature anomalies

Figure IX.1, copied from reference [IX.1], shows a graph of the monthly temperature deviations per year relative to the worldwide mean global temperature for that year since 1880. The separation of the curves has been realized by adding the related *long-term* increase of the worldwide mean global temperature during that year. As a result the curve for the year 2017 is drawn about 1 °C higher than the curve for 1880. See note* regarding the original source: reference [IX.2].

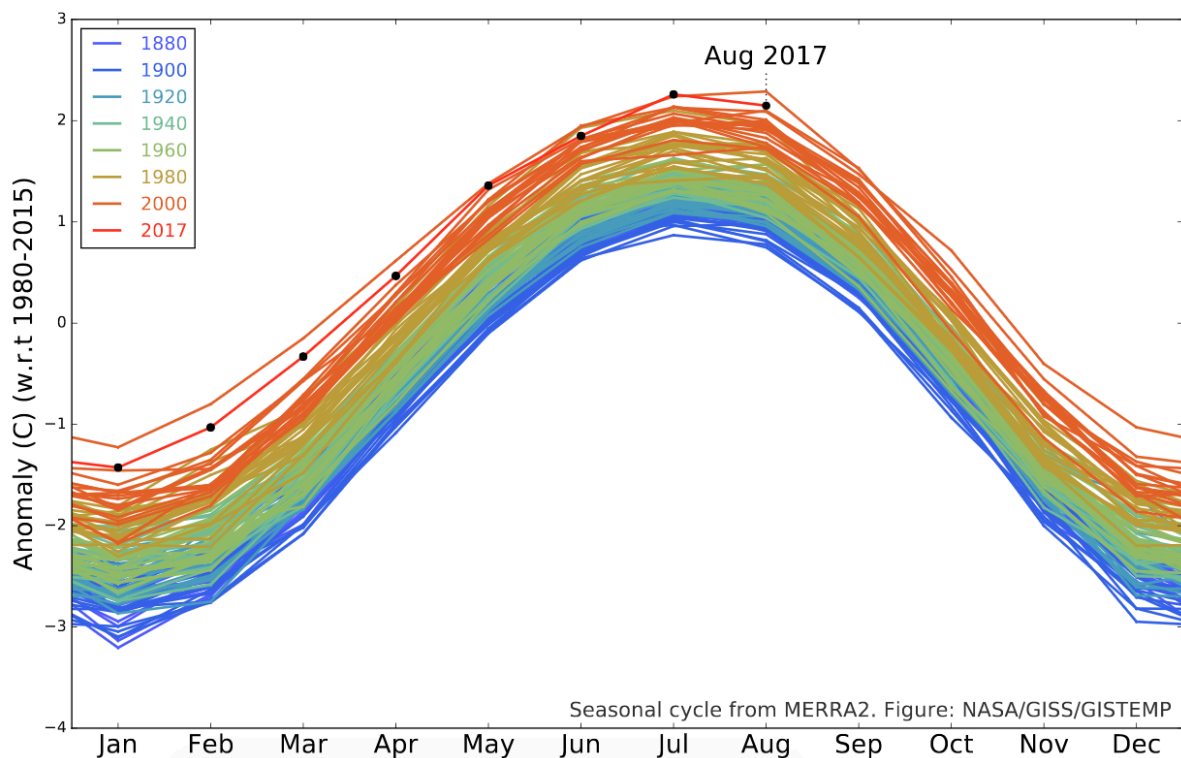


Figure IX.1: GISTEMP Seasonal Cycle since 1880

Possible background for the presented anomalies.

Reference [IX.3] presents that during the summer the rise in temperature around the North pole (between 60° and 82.5° latitude) is significantly higher than the fall in temperature around the South pole in the same months. A similar phenomenon occurs between 32.5° and 50° latitude. The graphs of these anomalies are shown in the figures IX.2 and IX.3. The blue line shows the mean value during the period 1980–1989 and the red line during the period 2000–2009. The curves prove that this phenomenon is perfectly consistent.

* Reference [IX.2] should have shown such anomalies, but doesn't anymore. The person who is responsible for this data has been sent an email for clarification. It has been admitted that this data has been removed, but a clarification is not given, not even after two other attempts.

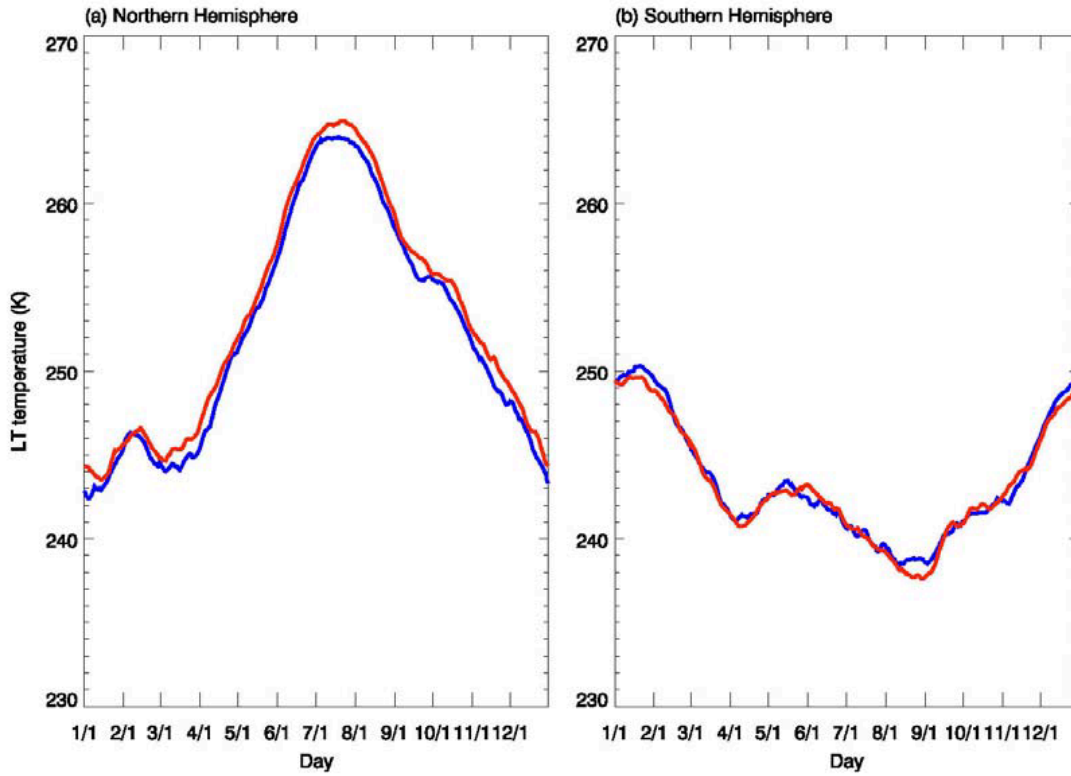


Figure IX.2: Temperature measurements between 60° and 82.5° latitude

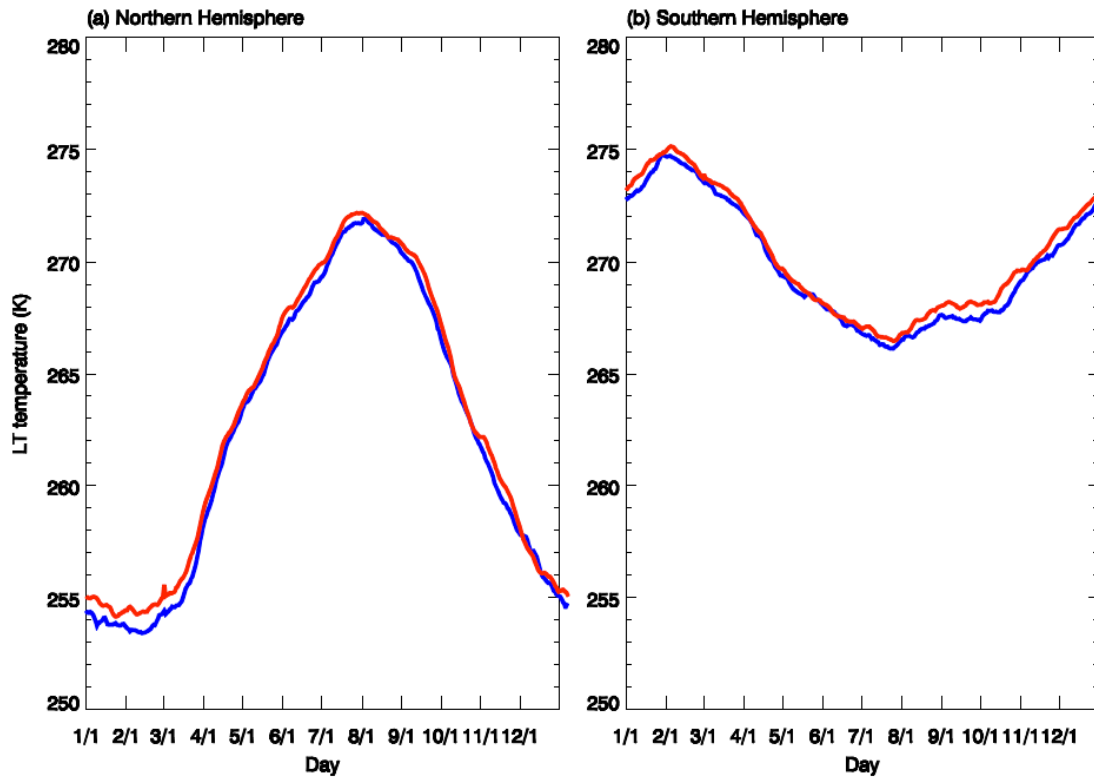


Figure IX.3: Temperature measurements between 32.5° and 50° latitude

These graphs have been converted into data shown in Table IX.1 in the columns marked with NH and SH. Although the differences between the red and blue lines are very small, the mean value is presented.

month	latitudes (60° to 82.5°)		latitudes (32,5° to 50°)		latitudes	dev. latitudes
	NH	SH	NH	SH	mean °C	mean
	temp	temp	temp	temp	-15,8	
1	243,4	249,5	255,0	273,1	-17,8	-2,0
2	245,6	249,2	254,0	274,8	-17,1	-1,3
3	244,6	245,4	255,0	273,5	-18,4	-2,6
4	246,0	241,6	258,6	272,1	-18,4	-2,6
5	251,5	242,6	263,3	269,4	-16,3	-0,5
6	257,1	243,0	267,1	268,0	-14,2	1,6
7	263,6	240,7	269,5	266,9	-12,8	3,0
8	264,0	239,1	271,9	266,7	-12,6	3,2
9	258,9	238,1	270,6	267,8	-14,2	1,6
10	255,6	240,9	266,9	269,2	-14,9	0,9
11	252,0	242,3	262,0	271,0	-16,2	-0,4
12	248,5	246,1	258,0	272,8	-16,7	-0,9

Table IX.1

The variable “Latitudes mean” shows the mean values of all the 4 temperatures on its left side in °C. The green value on top is the mean value of these mean values, used to calculate “dev. latitudes mean”. The top-top value of this variable is 5 to 6 °C, so significantly higher than the top-top values of 4 °C in figure IX.1. That is logical, because the variable “Latitudes mean” is a very poor representative of the *globally mean* temperature. The last one is the mean value of thousands of stations on the global surface. But their respective maximum and minimum value are in the same months (Jul-Aug resp. Dec-Jan).

This investigation thus learns that the monthly global temperature anomalies, as shown in figure IX.1, are strongly related to the orientation of the Earth’s rotation axis relative to the Sun. However, it doesn’t explain yet in more detail what happens on Earth during summer and winter, in NH, resp. SH, that causes these mutual significant differences. More details will be presented in the next section.

The map in figure IX.4 shows perfectly the seasonal temperature differences between NH and SH.

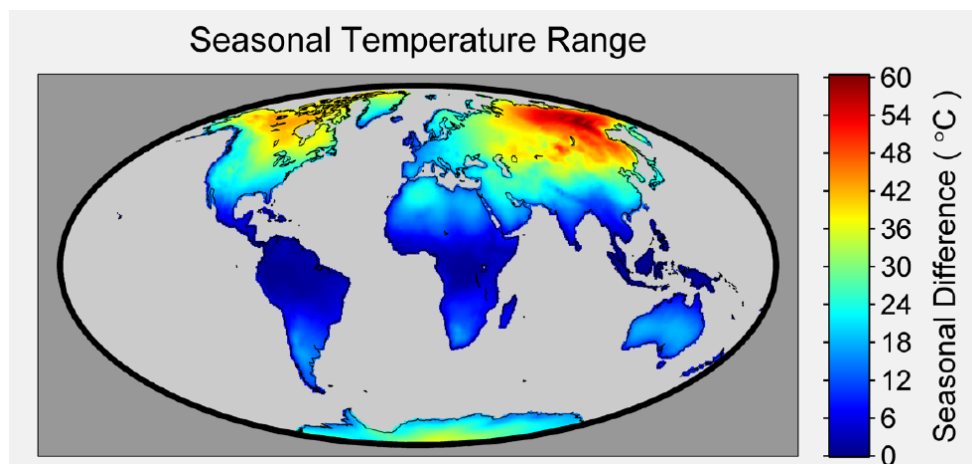


Figure IX.4: “Using the Berkeley Earth Surface Air Temperature (SAT) dataset the seasonal temperature range was calculated over the entire land surface of the globe. For the purposes of this map the seasonal range was defined as the difference between the warmest month and the coolest month. The difference ranges from a low of 0 degrees C in equatorial regions to a high of 60 degrees C in north eastern Russia. While not as dramatic as the ranges found in Siberia, the seasonal range in northern Canada is also large.”

This phenomenon is also known as Polar amplification, reference [IX.4]. Given the large difference between North and South Pole the phenomenon has been split into Arctic and Antarctic amplification. The explanation is based on the Greenhouse Model, without giving an explanation for the large difference between Arctic and Antarctic amplification: “Polar amplification is the phenomenon that any change in the net radiation balance (for example greenhouse intensification) tends to produce a larger change in temperature near the poles than the planetary average.”

IX.2 Monthly CO₂ anomalies

Reference [I] shows the monthly records of the CO₂-concentration in the atmosphere in ppm since 1958. It has been used to make a graph of this anomaly averaged over the total period of measurements. Figure IX.5 shows this graph as well as the monthly temperature anomalies, also as averaged values over the whole period of measurements*. The curves have been made symmetrical around zero by subtracting the yearly mean value over the respective periods.

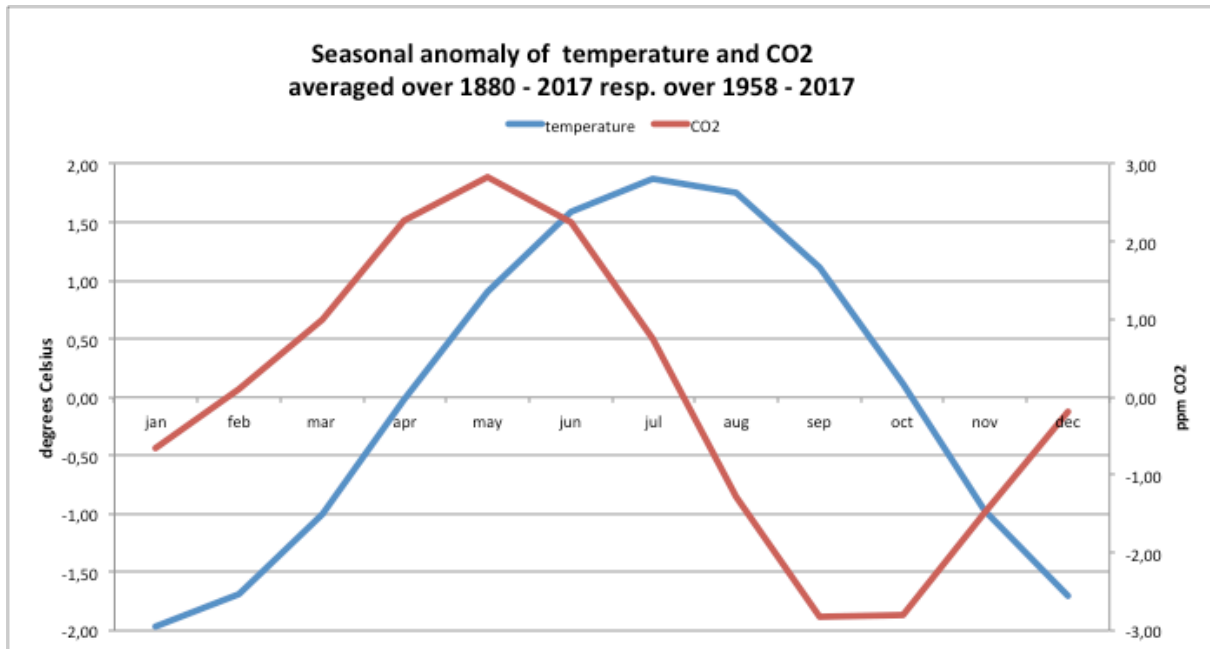


Figure IX.5: Mean monthly CO₂ and global temperature anomalies w.r.t. yearly mean values

Figure IX.5 shows that during the summer of the NH (around July) the globally averaged CO₂ concentration starts to become lower than the yearly mean value. This can possibly be understood as follows. A property of plants is that they grow more during warm periods than during cold periods and that they thus absorb more CO₂ during a growing period. During the summer of the NH it is winter on the SH. However the SH has by far less area where plants grow and at all these areas it never becomes cold, because they are all located closer to the equator. So the plants at the SH will not create a significant anomaly in the absorption of CO₂ during a year. As a result the globally mean value is season dependent, without any relation with the long-term trend of this variable

The question remains what the fundamental cause of the monthly temperature anomaly might be.

The generally accepted idea is that the Sea absorbs more heat than land does. Given the fact that the SH contains by far more water than the NH, the temperature of the atmosphere at SH increases less during summer at SH (Oct-Feb) than this temperature does at NH during summer at NH (Apr-Aug).

Given these argumentations the conclusion must be that the seasonal anomalies don't have any relation with the long-term increase of the yearly averaged global atmospheric temperature, neither of the yearly averaged CO₂ concentration in the atmosphere.

* The curve in figure IX.5 is based on data that was available at the original site until the end of 2017!

X Global Mean Sea Level until 2100

X.1 Introduction

Global Mean Sea Level is a hot topic nowadays, because maybe we will eventually drown in the oceans. The most intricate models for its increase in the future have been created and will be created, some of them leading to the most worst thinkable scenario in 2100. See for example reference [X.1].

Several organisations realize data sets for the GMSL. They have all been asked in 2018 for numerical data. The only one that did react fast as well as with appropriate data was CSIRO, indirectly shown in [X.2].

X.2 Mathematical expression for CSIRO measurements

The CSIRO data, presented as monthly mean values in mm, have been transformed to yearly mean values in cm. After that the values have been corrected with a constant value in order to start at 0 cm in 1880. Figure X.1 shows the measured Sea level rise, as well as the corresponding fitted exponential function:

$$SL(t) = -10.8 + 1.7 \cdot 10^{-6} \cdot \exp(t/120) \quad \text{cm} \quad (6)$$

The figure proves that this function fits the measured values perfectly. The standard deviation of the measured values with respect to this curve has been calculated as 0.65 cm.

In November 2021 satellite data for the period 1993 – 2019 has been added, using the graph in ref. [X.3].

The calculations carried out in chapter VI show that the GMSL rise, only as a result of the expansion of the water during the past 150 years, is 9.3 cm. The measured increase is about 22.5 cm. The remaining 13 cm must be the result of the melting of the snow on the mountains on the mainland and of the snow on both poles. Not of the melting of the *ice* on and around the poles, because when ice melts, its volume decreases by 10%. On the basis of the currently measured GMSL rise, it is therefore grossly exaggerated to predict that we have to take meters of increase into account. Figure X.1 shows that even if the prevailing increasing trend of global warming is maintained over the next 100 years, the GMSL will rise only 30 cm from the current level.

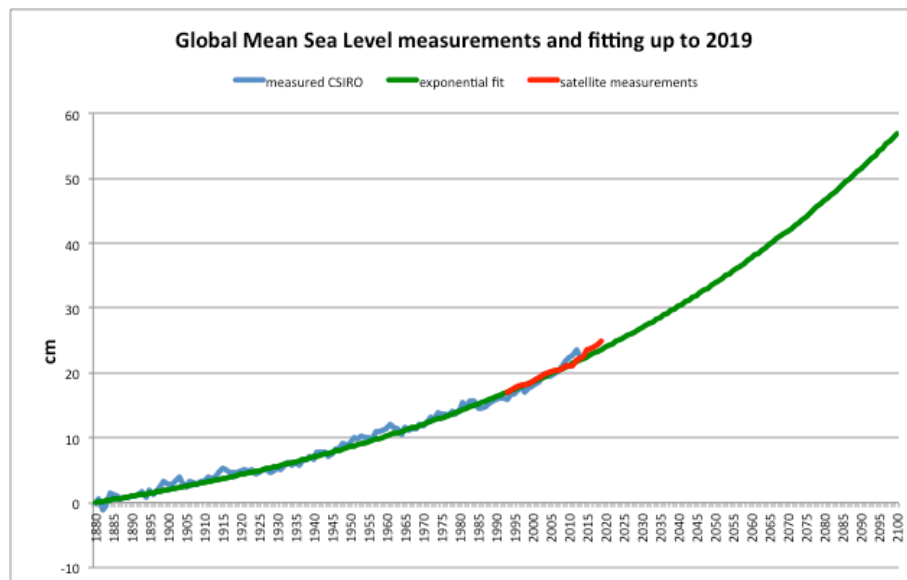


Figure X.1 All satellite data is corrected with +0.9 cm w.r.t. the fitted CSIRO value in 1993

The observation that by far the largest part of the GMSL rise must have been caused by snowmelt, forces us to consider more closely its possible influence on Sea's temperature increase. The snowmelt at the poles results in water of the same temperature as the water of the sea around the poles. The snow melting on the mainland is heated during the time it flows to the Sea. It is heated until roughly the temperature of the atmosphere. However the amount of Seawater on Earth is much larger than the amount sweet water. Its temperature, roughly equal to atmosphere's temperature, can therefore not have significant influence on Sea's temperature. All Sea's heat energy increase must have been accomplished by the geothermal flux.

Conclusions

1. The long-term-trends of the variables: atmospheric CO₂ concentration, global temperature, world population and globally applied power by mankind, can all four truthfully be represented by the function: $y_i = c_i + a_i \cdot \exp(t/b)$, with b the same for all of them and equal to 61 years.
2. Superimposed on this trend the global temperature turned out to have a perfect sinusoidal variation with a period of 64 years and an amplitude of 0.1 °C. This variation is many times used as argument against the validity of the Greenhouse Model, but it hasn't anything to do with global warming.
3. Given their same curvature, these variables can all simply be expressed as function of each other. For example: global temperature equals $13.5 \text{ }^\circ\text{C} + 0.05 \text{ (}^\circ\text{C/TW)} \cdot \text{globally applied power (TW)}$.
4. The just shown expression and the calculation of the heat capacity of the atmosphere has eventually lead to the evidence that the increase of atmosphere's temperature is caused by the worldwide consumed energy, *of whatever kind*. The here called Living Room Model.
5. The alleged power density of the Greenhouse Model in 2010 is 0.6 W/m². It has been proven that this number is even a factor 1.5 too low. Taking the correct number it is about 30 times higher than the one of the Living Room Model.
6. The Greenhouse Model claims that the Sea is heated by the net difference between Sun's heating radiation during day-time and Earth's cooling radiation during night-time. But this claim has never been validated by means of measurements of these radiations. Its alleged enormous power density has only been created in order to try to explain the heating of the Sea.
7. It has been shown that the heating of the Sea cannot be caused by a heating top down, but must take place bottom up, in this case by the geothermal heat flux of Earth's core.
8. Permafrost is also affected by the geothermal heat flux in the same way as the Sea is heated by this phenomenon.
9. The so-called thermohaline circulation is most likely caused by the bottom up heating of the Sea by means of the geothermal heat flux and should therefore not be used as the explanation of the top down heating of the Sea, as done in the Greenhouse Model.
10. A convincing argument against the Greenhouse Model is the observation of so-called Hot Spots on Earth. The only way to explain them is to apply the Living Room Model.
11. It has been proven, based on 3 different kinds of observations, that the atmosphere absorbs 10 ppm more CO₂ per °C rise of its temperature, here called the Reverse Greenhouse Effect. The existence of this phenomenon excludes the existence of the Greenhouse Effect, because the simultaneous existence would lead to an 'explosive' increase of both variables.
12. The enormous temperature difference at the surfaces of Mars and Venus doesn't have anything to do with Greenhouse effects, but is caused by the geothermal flux of these planets in combination with the enormous difference in isolation to space of the respective atmospheres.
13. Given these evidences the Greenhouse Model has to be rejected in favour of the Living Room Model.
14. An exponential fit has been applied to the Global Mean Sea Level measurements. Extrapolation to the year 2100 shows a rise of ~30 cm relative to the present year, assumed that the global warming keeps rising with the same curvature, so up to an increase of 4 °C in the year 2100.

Appendix 1 Mathematical background of the polynomial and exponential curve fitting

1.1 Polynomial curve fitting

Polynomial fitting means the fitting of the measured data y_n , as function of the variable x_n , to a polynomial y of order k : $y = \sum_0^k a_i x^i$, in such a way that the sum R (esiduals) of the quadratic deviations between the measurements y_n and y is minimal. The variable x is an arbitrary value inside as well as outside the original range of x_n , just like y is in relation to y_n .

$$R = \sum_{i=1}^n \{y_i - y\}^2 = \sum_{i=1}^n \{y_i - (a_0 + a_1 x_i + \dots + a_k x_i^k)\}^2 \quad \text{N.B. The symbol } \Sigma \text{ is exclusively assigned to } i.$$

For minimization the following relations have to be fulfilled:

$$\begin{aligned} \partial R / \partial a_0 &= -2 \sum_{i=1}^n \{y_i - (a_0 + a_1 x_i + \dots + a_k x_i^k)\} = 0 \\ \partial R / \partial a_1 &= -2 \sum_{i=1}^n x_i \{y_i - (a_0 + a_1 x_i + \dots + a_k x_i^k)\} = 0 \\ \partial R / \partial a_2 &= -2 \sum_{i=1}^n x_i^2 \{y_i - (a_0 + a_1 x_i + \dots + a_k x_i^k)\} = 0 \\ &\vdots \\ \partial R / \partial a_k &= -2 \sum_{i=1}^n x_i^k \{y_i - (a_0 + a_1 x_i + \dots + a_k x_i^k)\} = 0 \end{aligned}$$

These relations can be written as:

$$\begin{aligned} a_0 \sum_{i=1}^n 1 + a_1 \sum_{i=1}^n x_i + \dots + a_k \sum_{i=1}^n x_i^k &= \sum_{i=1}^n y_i \\ a_0 \sum_{i=1}^n x_i + a_1 \sum_{i=1}^n x_i^2 + \dots + a_k \sum_{i=1}^n x_i^{k+1} &= \sum_{i=1}^n x_i y_i \\ &\vdots \\ a_0 \sum_{i=1}^n x_i^k + a_1 \sum_{i=1}^n x_i^{k+1} + \dots + a_k \sum_{i=1}^n x_i^{2k} &= \sum_{i=1}^n x_i^k y_i \end{aligned}$$

In matrix format:

$$\begin{array}{cccccc} \sum_{i=1}^n 1 & \sum_{i=1}^n x_i & \dots & \sum_{i=1}^n x_i^k & a_0 & \sum_{i=1}^n y_i \\ \sum_{i=1}^n x_i & \sum_{i=1}^n x_i^2 & \dots & \sum_{i=1}^n x_i^{k+1} & a_1 & \sum_{i=1}^n x_i y_i \\ \vdots & \vdots & \vdots & \vdots & \vdots & \vdots \\ \sum_{i=1}^n x_i^k & \sum_{i=1}^n x_i^{k+1} & \dots & \sum_{i=1}^n x_i^{2k} & a_k & \sum_{i=1}^n x_i^k y_i \end{array} \quad X =$$

Shortly written as: $M_x \cdot \underline{a} = M_y \cdot \underline{y}$, with \underline{a} and \underline{y} to be read as a column vectors.

The matrix M_x can be composed by the product of the 2 matrices: $M^T \cdot M$, with M^T the transpose of M and M and M^T as shown below.

$$\begin{array}{cccc|cccc} & \text{M (k x n)} & & & & \text{M}^T \text{ (n x k)} & & \\ 1 & x_1 & \dots & x_1^k & 1 & 1 & \dots & 1 \\ 1 & x_2 & \dots & x_2^k & x_1 & x_2 & \dots & x_n \\ \vdots & \vdots & \vdots & \vdots & \vdots & \vdots & \vdots & \vdots \\ 1 & x_n & \dots & x_n^k & x_1^k & x_2^k & \dots & x_n^k \end{array}$$

It turns out that $M^T \cdot \underline{y} = M_y \cdot \underline{y}$, as defined above, so $M_y = M^T$. As a result: $M^T \cdot M \cdot \underline{a} = M^T \cdot \underline{y}$

Both sides 'left side multiplied' by $(M^T \cdot M)^{-1}$ results in: $(M^T \cdot M)^{-1} \cdot M^T \cdot M \cdot \underline{a} = (M^T \cdot M)^{-1} \cdot M^T \cdot \underline{y}$.

Given: $(M^T \cdot M)^{-1} \cdot M^T \cdot M = I$, it follows that $\underline{a} = (M^T \cdot M)^{-1} \cdot M^T \cdot \underline{y}$, showing the requested coefficients a_i .

Note:

Calculating the check $(M^T \cdot M)^{-1} \cdot M^T \cdot M = I$, the result strongly departs from that unity matrix I for orders greater than 6, due to the restricted number length of Excel. However the 8th and 9th order polynomials still seem to be calculated good enough in the current investigations, given their strong similarity.

1.2 Exponential curve fitting

Exponential curve fitting is here meant to be the use of 3 points of measurement out of a collection of measurement data (here as function of time), in which a clear tendency is visible. The 3 measurements are used for the solution of the 3 variables a, b and c in the function $y = c + a \cdot \exp(t/b)$. The variable t will represent the year under consideration. As a result the dimension of b is also “year”.

Given the measuring points: (t_1, y_1) , (t_2, y_2) en (t_3, y_3) the solution of the constant c is as follows:

$$y_1 - c = a \cdot \exp(t_1/b)$$

$$y_2 - c = a \cdot \exp(t_2/b)$$

$$y_3 - c = a \cdot \exp(t_3/b)$$

$$\ln(y_1 - c) = \ln(a) + t_1/b$$

$$\ln(y_2 - c) = \ln(a) + t_2/b$$

$$\ln(y_3 - c) = \ln(a) + t_3/b$$

$$\ln(y_1 - c) - \ln(y_2 - c) = (t_1 - t_2)/b$$

$$\ln(y_1 - c) - \ln(y_3 - c) = (t_1 - t_3)/b$$

$$b = (t_1 - t_2) / \{\ln(y_1 - c) - \ln(y_2 - c)\}$$

$$b = (t_1 - t_3) / \{\ln(y_1 - c) - \ln(y_3 - c)\}$$

c can only be solved numerically by means of an iteration process, applied to the function :

$$(t_1 - t_2) / \{\ln(y_1 - c) - \ln(y_2 - c)\} - (t_1 - t_3) / \{\ln(y_1 - c) - \ln(y_3 - c)\} = 0$$

$$b = (t_1 - t_3) / \{\ln(y_1 - c) - \ln(y_3 - c)\}$$

$$a = (y_2 - c) / \exp(t_2/b)$$

In this report an essential approach is that several times the fitting to other measured variables is started with the same b as found for the CO₂ concentration. In such a situation the solving of a and c is as follows:

$$B_i = \exp(t_i/b)$$

$$y_1 = c + a \cdot B_1$$

$$y_3 = c + a \cdot B_3$$

$$y_1 - y_3 = a \cdot (B_1 - B_3)$$

$$a = (y_1 - y_3) / (B_1 - B_3)$$

$$c = y_1 - a \cdot B_1$$

Appendix 2 Calculation of the heat capacity of the atmosphere

2.1 Temperature constant as function of height

The specific heat capacity of air at 0 °C and 1 bar is 1000 J/kg/K. The specific weight of such air (sw_0) is 1.3 kg/m³. Multiplication of these quantities leads to its specific volumetric heat capacity as 1300 J/m³/K.

Quote from: https://en.wikipedia.org/wiki/Atmospheric_pressure :

” Altitude variation

Pressure on Earth varies with the altitude of the surface;.....

$$p(h) \approx p_0 e^{-Mgh/RT}$$

with:

p_0	Sea level standard atmospheric pressure	101325 Pa	
h	Altitude	m	
M	Molar mass of dry air	0.029 kg/mol	
g	Earth-surface gravitational acceleration	9.8 m/s ²	
R	Universal gas constant	8.31 J/(mol·K)	
T	Sea level standard temperature	288.15 K	”

In stead of $p(h)$ the variable $sw(h)$ can be chosen. Replacing the e-power function into e^{a-Ch} , with the boundary condition that $e^{a-Ch}=1$ for $h=r$ (r the radius of the Earth), this function becomes e^{Cr-Ch} .

The total mass of air in the atmosphere can now be calculated as: $sw_0 \int_r^\infty e^{Cr-Ch} \cdot O(h) \cdot dh$, with $O(h)=4\pi h^2$.

The function to be calculated is therefore: $4\pi \cdot sw_0 \cdot e^{Cr} \cdot \int_r^\infty e^{-Ch} \cdot h^2 \cdot dh$.

After applying twice partial integration to $\int_r^\infty e^{-Ch} \cdot h^2 \cdot dh$ the result is $-C^{-1} \cdot e^{-Ch} \cdot (h^2 + 2C^{-1}h - 2C^{-2}) \Big|_r^\infty$

A few calculations of $e^{-Ch} \cdot h^2$ learn that the value of this integrand is zero for $h \rightarrow \infty$.

The result for the total mass of the atmosphere thus is:

$$4\pi \cdot sw_0 \cdot e^{Cr} \cdot C^{-1} \cdot e^{-Cr} \cdot (r^2 + 2C^{-1}r - 2C^{-2}) = 4\pi \cdot 1.3 \cdot C^{-1} \cdot (r^2 + 2C^{-1}r - 2C^{-2})$$

The constant $C^{-1} = RT/Mg$ equals: $8.31 \cdot 288 / (0.029 \cdot 9.8) = 8420$ m.

Because the temperature is expressed in Kelvin, the sensitivity of that parameter is low.

The radius r of the Earth is 6371000 m. With $2C^{-1}r - 2C^{-2} \ll r^2$, the result of the integral is $4\pi \cdot 1.3 \cdot C^{-1} \cdot r^2$.

So the total mass of the atmosphere is $5.6 \cdot 10^{18}$ kg.

This calculation forms the essential basis for the calculation of the total heat capacity of the atmosphere. The mass calculated in this way is also a check on the method used. This check is that the total mass can easily be calculated too as follows:

The atmospheric pressure on the Earth's surface is 101325 Pa = $1.013 \cdot 10^5$ N/m² or kg m⁻¹ s⁻².

The surface of the Earth is $5.1 \cdot 10^{14}$ m². The total mass of air in the atmosphere is therefore $1.013 \cdot 10^5 \cdot 5.1 \cdot 10^{14} / g$. With $g = 9.8$ ms⁻² resulting in $5.3 \cdot 10^{18}$ kg.

The atmospheric heat capacity thus is $(5.3 \text{ á } 5.6) \cdot 10^{18}$ kg \cdot 1000 J/kg/K = $(5.3 \text{ á } 5.6) \cdot 10^{21}$ J/K, neglecting the influence of its temperature as function of height.

This has been checked in the next section.

2.2 Temperature height dependant

The figure below shows how T depends on the height in the atmosphere.

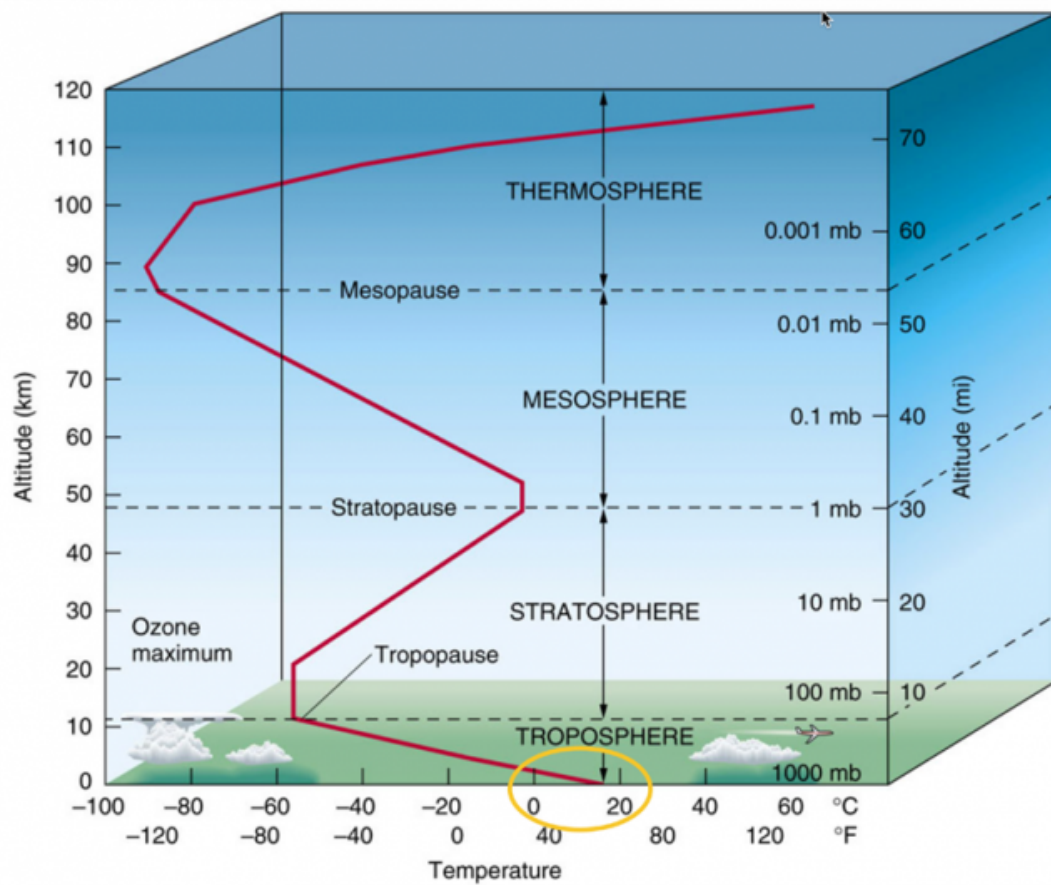


Figure Appendix 2

In order to check the influence of this variation the integral $4\pi \cdot sh_0 \int_r^\infty e^{-Ch} \cdot h^2 \cdot dh$, as used in the previous section, has now to be written as $4\pi \cdot sh_0 \int_r^\infty e^{C(h)(r-h)} \cdot h^2 \cdot dh$, with $C(h) = Mg/RT(h)$.

This integral has been calculated numerically in Excel in steps of 100 m and with $sh_0 = 1300 \text{ J/m}^3/\text{K}$.

The calculation is checked by taking T height independent and 288 K and for a maximum height of 120 km, in accordance with the maximum height shown in the figure above. The outcome is $5.6 \cdot 10^{21} \text{ J/K}$, so sufficiently in agreement with the analytical outcome.

Replacing the temperature in a height dependent one in accordance with the information shown in the figure above, the result is $4.6 \cdot 10^{21} \text{ J/K}$.

This outcome, together with the two outcomes in the previous section, presents a good reason to take as a rounded value for the heat capacity of the atmosphere the value $5 \cdot 10^{21} \text{ J/K}$.

Appendix 3 Impact of sustainable energy

3.1 Sun energy

The net electrical power generated by means of sun cells is 15 W/m^2 . Experience learns that a mean household of 3 persons in the prosperous part of the world can generate its own need for electrical purposes by means of 20 m^2 of sun cells. The heating of the house excluded. Including the heating would result in about 50 m^2 . So heating the houses with their own sun energy is impossible.

The need for electrical energy of the meant household is, exclusive the heating, 100 W per person. The prosperous part of the world population is roughly living in the 17 countries, mentioned at the end of section VIII.6, occupied by 5 billion persons. These prosperous 5 billion persons as a result need 0.5 TW power, exclusive the heating. Such a power is a negligible fraction of the worldwide required power of 20 TW . Nature would worldwide be destroyed, if such a power would have to be generated by sun cells.

3.2 Wind energy

The drawing in figure Appendix 3, copied from ref. [A], shows the power of the worldwide generated wind energy. It presents in 2014 a growth of 51 GW , so 0.05 TW/year , in terms of *capacity!*

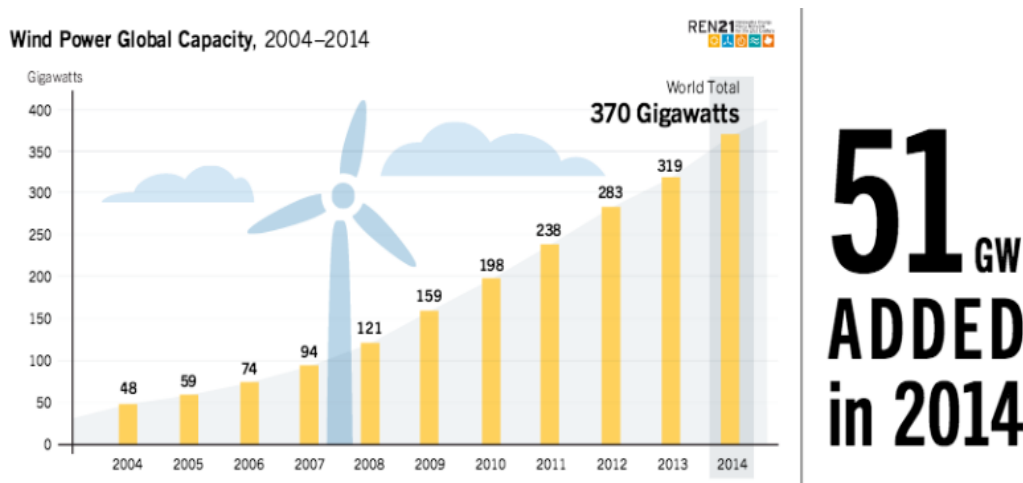


Figure Appendix 3

The expression “ Wind Power Global Capacity” is misleading. It should have been presented as Globally *Installed* Wind Power. The generally accepted net power is 20% of its installed power, so the presently net wind power is $< 0.1 \text{ TW}$. Completely negligible w.r.t the global need of about 20 TW at this moment.

The derivative of (4) in chapter V shows a prevailing annual growth in applied power of 0.3 TW/year . The annual growth of *net* wind power is 0.01 TW/year , so also completely negligible w.r.t. the applied one.

3.3 Earth heat energy

Suppose the worldwide mean family consists of 3 persons and suppose each family needs a power of 500 W to heat its house. As soon as the world population would consists of 3 billion of such families, the required total power to heat all the houses on the world would be 1.5 TW . That is a negligible fraction of the total need at that time: 23 TW . So even in the most extreme, and at the same time most unrealistic, situation that each house on the world would be heated by means of Earth heat energy, only a negligible part of the worldwide required power would be generated by such a kind of sustainable energy.

But to top it all of. As presented in the Living Room Model, whatever kind of energy is applied it is all converted into heat. So applying sustainable energy will not solve the problem of the increasing global temperature at all.

Appendix 4 The World Population in the Past and in the Future

4.1 Introduction

Given the proven validity of the Living Room Model, it has to be concluded that the global heating problem is a symptom of a much more fundamental problem: the worldwide overpopulation.

The world population is known through censuses, but up to 1950 only by approximation. The more accurate the past is known, the better the future can be predicted therefrom. The approximations, together with the more precise-looking counts after 1950, are processed into a natural looking curve for the period 1800 up to now in chapter III. Using the mathematical expression for this curve, predictions can be calculated for the future. In addition a simple model has been realized in this appendix for the growth of a population. Mutual comparison of the two curves results in interesting conclusions, of which the most important one is that the solution of the climate problem must be sought in the reduction of the world population.

4.2 Applied growth model of a population

Given the fact that a large number of statistical variables permit to work with (only) averages, the following simple model of the growth of a population is established, based on the following assumptions:

- 1 The world population is made up of N humans.
- 2 There are $N/2$ male and $N/2$ female humans.
- 3 Each human dies at age L , where L is the average age of the N humans.
- 4 The age of humans is distributed evenly, so there are N/L humans by age.
- 5 Each couple gets at a certain age x children, of which S survive to procreate.
The variable S thus is the net result of the birth and of the death among youth.

From this model it follows directly that if $S = 2$ the population is not growing nor declining.

Indeed, every year N/L humans die and every year $S \cdot (N/2)/L$ humans procreate.

At a constant population, these two expressions are equal.

This model is realized in an Excel program in which the increase and decrease of the population in each year is calculated from the previous year. By adding this net result of the population growth to the population in the previous the population of the present year is obtained. In symbolic form:

Year	decrease	increase	population
Y-1			N_{Y-1}
Y	$S \cdot (N_{Y-1}/2)/L$	N_{Y-1}/L	$N_{Y-1} + S \cdot (N_{Y-1}/2)/L - N_{Y-1}/L (=N_Y)$

In order to verify that this model fits somewhat with actual counts/estimates (henceforth the sake of brevity from now on referred to as observations) the graph from reference [1] is taken as the reference. This graph is based on a curve fitting of the available observations. This curve fitting is based on the model $y = c + a \cdot \exp(t/b)$, with the symbol t representing the year and y the number of humans. With the aid of this expression the number of humans outside the period of observation can be calculated too for each year. The period 1800-2100 is chosen here.

The variables L and S are, by trial and error, adjusted in such a way that the populations in 2100 in both models are equal. The initial value N_{1800} of the growth model is of course selected equal to the initial value of the observations. Figure Appendix 4.1 shows this result for $L = 60$ and $S = 3.5$.

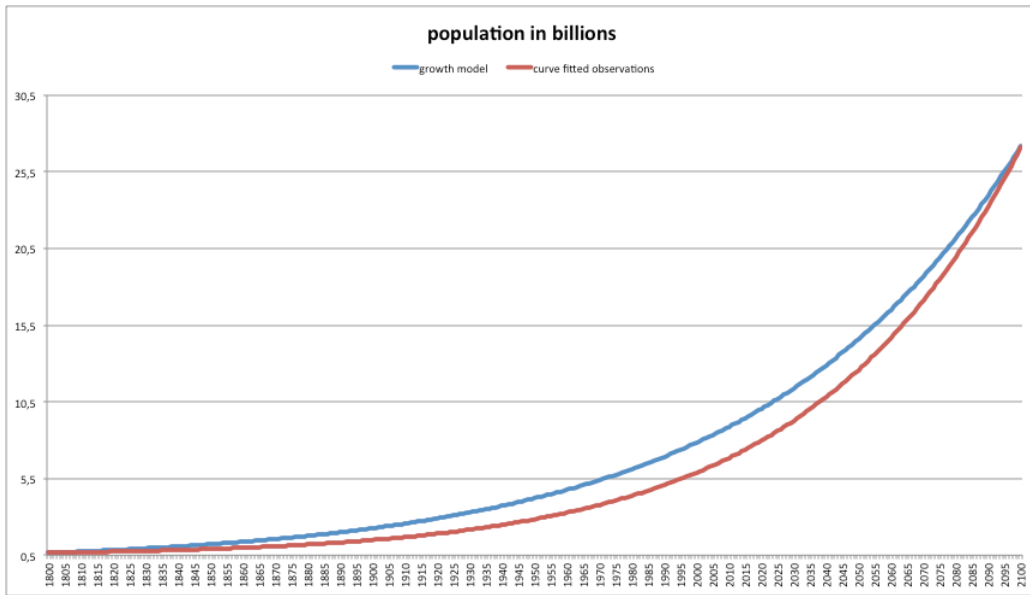


Figure Appendix 4.1 with $L = 60$ and $S = 3.5$ in the growth model

Subsequently, the growth model is adjusted by making both variables L and S as a function of time. L in the year 1800 is, of course, chosen to be smaller than in the year 2100. In-between it increases linearly with time. For S basically the same is done.

These variables are now labelled: L_{1800} and L_{2100} , respectively S_{1800} and S_{2100} .

Figure Appendix 4.2 shows the well-fitting result for: $L_{1800} = 60$, $L_{2100} = 75$, $S_{1800} = 3$ and $S_{2100} = 4.4$. For information: the values $L_{1800} = 60$, $L_{2100} = 70$, $S_{1800} = 3$ and $S_{2100} = 4.27$ result in an equally perfect fit!

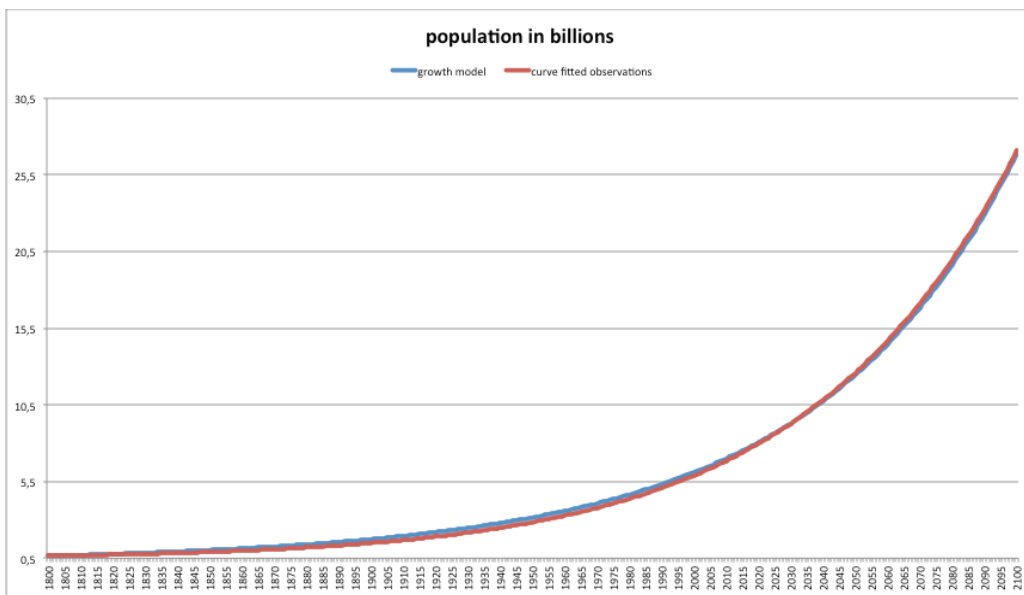


Figure Appendix 4.2 with $L_{1800} = 60$ and $L_{2100} = 75$, resp. $S_{1800} = 3$ and $S_{2100} = 4.4$ for the growth model

Based on this well-fitting growth model with the observations, this model is frozen for the period 1800-2017 in order to investigate what will be the development of the population in the future, varying only the variable S , so only S_{2100} . The reason for this is that variable L is found to be much less sensitive. It turns out that in 2017 the variable S equals 4.008. Starting from this value, S decreases linearly down to S_{2100} in the year 2100. Figure Appendix 4.3 shows the results for $S_{2100} = 2, 1$ and 0 .

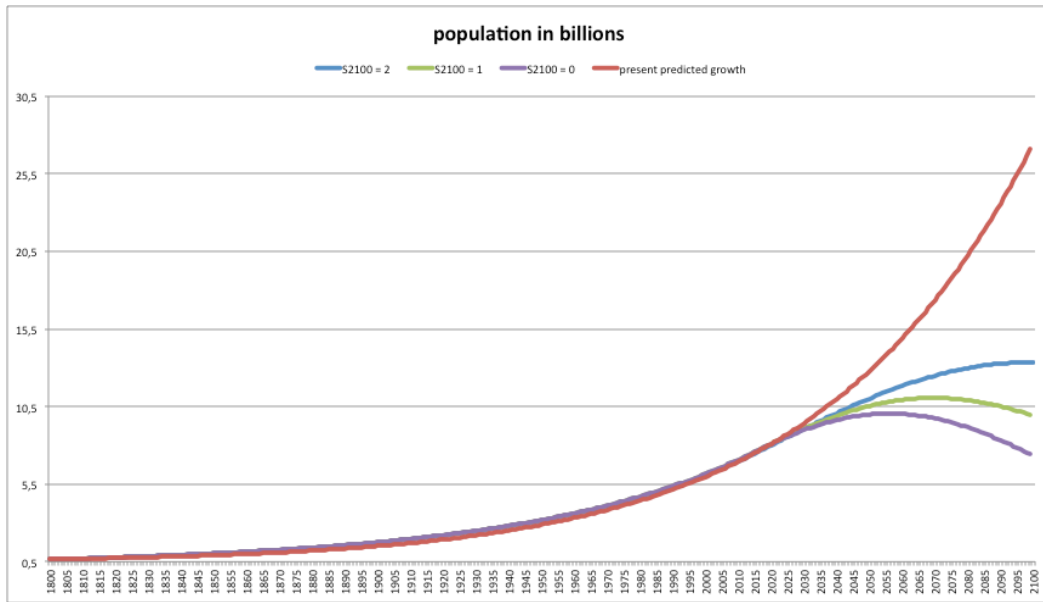


Figure Appendix 4.3, with 3 possible growth scenarios in relation to the current growth

Resume

- 1 With the described simple growth model it is possible to reproduce perfectly the observed world population from the year 1800 to the present year.
- 2 The applied parameter values for the average age L and the average number S of people per pair that procreates again, all the way look realistic: $L_{1800} = 60$ and $L_{2017} = 71$ years, resp. $S_{1800} = 3$ and $S_{2017} = 4$. The increase of the latter parameter is representative of the global average increased human health.
- 3 The three possible future growth scenarios all show that the current one rises so steeply that only a drastic reduction of the variable S , translated into a drastic decrease of the global birth rate, can save nature on Earth and as a result mankind.

Epilogue

The amount of heat in the atmosphere has been $15 \cdot 10^{23}$ J for at least thousands of years.

The increased amount of heat in the atmosphere during the past 150 years is $5 \cdot 10^{21}$ J.

In comparison to the existing heat thus an increase of only 3 pro mille.

The amount of heat in the Sea has been $15 \cdot 10^{26}$ J for at least thousands of years.

The increased amount of heat in the Sea during the past 150 years is $64 \cdot 10^{22}$ J.

In comparison to the existing heat thus an increase of only 0.4 pro mille.

The crucial question is: is such a heating of the atmosphere and the Sea really disastrous for Earth's nature and for mankind?

Should mankind in the first place not concentrate on reduction of the destruction and the pollution of nature?

References

- [I] ftp://aftp.cmdl.noaa.gov/products/trends/co2/co2_mm_mlo.txt
- [II] <http://climate.nasa.gov/vital-signs/global-temperature/>
- [III] https://en.wikipedia.org/wiki/World_population#/media/File:World_population_v3.svg
- [IV] http://www.theoil drum.com/files/world-energy-consumption-by-source_1.png
- [VI.1] <https://advances.sciencemag.org/content/3/3/e1601545>
- [VI.2] http://assets.climatecentral.org/pdfs/March2016_HeatContentSeaLevel_WMO.pdf
- [VII.1] <https://Earthobservatory.nasa.gov/features/EnergyBalance>
- [VII.2] <https://agupubs.onlinelibrary.wiley.com/doi/10.1029/2021GL093047>
- [VII.3] https://www.umweltbundesamt.de/sites/default/files/medien/1968/publikationen/co2_emission_factors_for_fossil_fuels_correction.pdf
- [VII.4] Climate and Atmospheric History of the Past 420,000 Years from the Vostok Ice Core, Antarctica
- [VIII.1] <https://www.statista.com/statistics/268750/global-gross-domestic-product-gdp/>
- [VIII.2] https://en.wikipedia.org/wiki/List_of_IMF_ranked_countries_by_GDP
- [VIII.3] <https://www.indexmundi.com/facts/indicators/AG.SRF.TOTL.K2/rankings>
- [VIII.4] The Netherlands is warming more than twice as fast as the global average temperature
- [IX.1] https://data.giss.nasa.gov/gistemp/graphs/graph_data/GISTEMP_Seasonal_Cycle_since_1880/graph.pdf
- [IX.2] https://data.giss.nasa.gov/gistemp/tabledata_v3/GLB.Ts+dSST.txt
- [IX.3] Satellite Global and Hemispheric Lower Tropospheric Temperature Annual Temperature Cycle
- [IX.4] https://en.wikipedia.org/wiki/Polar_amplification
- [X.1] https://www.researchgate.net/publication/314295190_A_high-end_sea_level_rise_probabilistic_projection_including_rapid_Antarctic_ice_sheet_mass_loss
- [X.2] http://www.cmar.csiro.au/sealevel/GMSL_SG_2011_up.html
- [X.3] <https://www.epa.gov/climate-indicators/climate-change-indicators-sea-level>
- [A] Renewable Energy Policy Network, 2015 © REN2 policy network